For Reference

NOT TO BE TAKEN FROM THIS ROOM

For Reference

NOT TO BE TAKEN FROM THIS ROOM

Ex libris
universitatis
albertaensis

University of Alberta
Printing Department

Digitized by the Internet Archive
in 2018 with funding from
University of Alberta Libraries

https://archive.org/details/martensiteintita00laks

THE UNIVERSITY OF ALBERTA

MARTENSITE IN TITANIUM, ZIRCONIUM AND TITANIUM-COPPER ALLOYS

A Thesis

Submitted to the Faculty of Graduate Studies

In Partial Fulfilment of the Requirements

for the Degree of MASTER OF SCIENCE

DEPARTMENT OF MINING AND METALLURGY

by

LAKSHMI PRAKASH SRIVASTAVA

EDMONTON, ALBERTA

SEPTEMBER 1961

ABSTRACT

A quenching unit in which small specimens may be heated to 1000 ^{o}C at a pressure of 10^{-5} mm of Hg, and quenched with a blast of high purity helium is described.

The Ms temperatures for titanium, zirconium, iron, titanium-43 pct. zirconium alloy and titanium-copper alloys up to 5.2 pct. copper have been determined. The Ms temperature decreases progressively with increasing copper content. The results of the present work agree with some of the earlier published results, disagree with others and provide new information about the mechanism of martensitic transformation.

ACKNOWLEDGEMENTS

The author is very grateful to Dr. J.G. Parr for his inspiration and for his capable guidance of the project, and to Prof. E.O. Lilge for his helpful departmental supervision.

He appreciates the assistance of several members of the Department, especially that of Messrs. Scott and Poling.

The author is particularly grateful to the Defence Research Board of Canada, whose financial assistance made the project possible.

TABLE OF CONTENTS

	Page
INTRODUCTION	1
LITERATURE REVIEW	3
EXPERIMENTAL	8
A. Apparatus	8
1. High Rate Quenching Unit	8
2. Specimen	16
B. Method	16
RESULTS	22
A. Transformation Temperatures	22
B. Metallographic	24
C. Hardness	24
D. Electrochemical	24
DISCUSSION	43
A. Titanium-copper Alloys	43
B. Titanium-zircinium Alloy	48
C. Martensite Transformation	50
SUMMARY AND CONCLUSIONS	69
BIBLIOGRAPHY	72
APPENDIX I - TABULATIONS OF THE TRANSFORMATION TEMPERATURES ON COOLING	79
APPENDIX II - SUMMARY OF THE TRANS-	89

Page

FORMATION TEMPERATURE ON REHEATING QUENCHED SPECIMENS

APPENDIX III- SUMMARY OF THE HARDNESS RESULTS ON TITANIUM-COPPER ALLOYS 94

APPENDIX IV- ELECTROCHEMICAL MEASUREMENTS ON TITANIUM AND ZIRCONIUM 96

Calculations 99

APPENDIX V - MATERIALS USED IN THE PROJECT 100

Titanium 101

Copper 101

Zirconium 102

Iron 103

LIST OF TABLES

		Page
TABLE 1	Ms Temperature , Critical Cooling Rate and the Transformation Temperature on reheating quenched samples of Titanium, Zirconium, Titanium-zirconium Alloy and Titanium-copper Alloys.	23
(APPENDIX I)		
TABLE 2	Transformation Temperatures of as-received pure Titanium	80
TABLE 3	Transformation Temperatures of Remelted pure Titanium (Cube Sample)	81
TABLE 4	Transformation Temperatures of Remelted pure Titanium (Ring Sample)	82
TABLE 5	Transformation Temperatures of Titanium 0.5 pct. copper and Titanium-1.0 pct. copper Alloys	83
TABLE 6	Transformation Temperatures of Titanium -1.5 pct. copper and Titanium-3.0 pct. copper Alloys	84
TABLE 7	Transformation Temperatures of Titanium -5.2 pct. copper Alloy	85
TABLE 8	Transformation Temperatures of Zirconium and Titanium-43 pct. zirconium Alloy	86
TABLE 9	Transformation Temperatures of pure Iron	87

Page

TABLE 10 Depression of the Ms Temperatures below the corresponding Equilibrium Temperatures in Titanium, Zirconium, Iron, Titanium-zirconium Alloy and Titanium-copper Alloys 88

(APPENDIX II)

TABLE 11 Transformation Temperature on reheating quenched samples of Titanium, Zirconium and Titanium-43 pct. zirconium Alloy 90

TABLE 12 Transformation Temperature on reheating quenched Samples of Titanium-0.5 pct. copper and Titanium-1.0 pct. copper Alloys 91

TABLE 13 Transformation Temperature on reheating quenched Samples of Titanium-1.5 pct. copper and Titanium-3.0 pct. copper Alloys 92

TABLE 14 Transformation Temperature on reheating quenched Samples of Titanium-5.2 pct. Alloy 93

(APPENDIX III)

TABLE 15 Hardnesses of Martensite and Diffusion Transformation Products in Titanium-copper Alloys 95

(APPENDIX IV)

TABLE 16 E.M.F. Measurements between Martensitic and Equiaxed Titanium 97

TABLE 17 E.M.F. Measurements between Martensitic and Equiaxed Zirconium 98

ILLUSTRATIONS

		Page
1.	Partial Titanium-copper Phase Diagram	4
2.	Photograph of the Apparatus Assembly	10
3(a)	Photograph of the Quenching Unit	11
3(b)	Photograph of the Heating Coil, Quenching Jet and the Specimen Assembly	12
4.	Diagram of the Quenching Assembly	13
5.	Photograph of the High Frequency Levitation Unit	17
6.	Photograph showing the Nature of the Cooling Curves	19
7.	Graph of the Transformation Temperature Vs. Cooling Rate of Titanium and Zirconium	25
8.	Graph of the Transformation Temperature Vs. Cooling Rate of Titanium-copper Alloys	26
9.	Graph of the Transformation Temperature Vs. Cooling Rate of Titanium-43 pct. zirconium Alloy	27
10.	Partial Titanium-copper Phase Diagram with determined Ms	28
11.	Graph of the Depression of Ms below the corresponding Equilibrium Temperatures in Titanium-copper Alloys	29
12.	Graph of the Hardness Vs. Composition in Titanium-copper Alloys	30
13.	Microstructure of Polished and Transformed (Slowly Cooled) Iron	31

		Page
14.	Microstructure of Polished and Transformed (Slowly Cooled) Titanium	31
15.	Microstructure of Polished and Transformed (Slowly Cooled) Zirconium	32
16.	Microstructure of Slowly Cooled Titanium-0.5pct. copper Alloy	32
17.	Microstructure of Polished and Transformed (Slowly Cooled) Titanium-1.5pct. copper Alloy	33
18.	Microstructure of Slowly Cooled Titanium-5.2pct. copper Alloy	33
19.	Microstructure of Slowly Cooled Titanium-8.0 pct. copper Alloy	34
20.	Microstructure of Polished and Transformed (Slowly Cooled) Titanium-43pct.zirconium Alloy	34
21.	Microstructure of Polished and Transformed (Martensitic) Iron	35
22.	Microstructure of Polished and Transformed (Martensitic) Titanium	35
23.	Microstructure of Polished and Transformed (Twinned) Titanium	36
24.	Microstructure of Polished and Transformed (Interlaced) Titanium	36
25.	Microstructure of Polished and Transformed (Martensitic) Zirconium	37
26.	Microstructure of Polished and Transformed (Martensitic) Titanium-0.5 pct. copper Alloy	37

		Page
27.	Microstructure of Martensitic Titanium-1.0pct. copper Alloy	38
28.	Microstructure of Polished and Transformed (Martensitic) Titanium-5.2pct. copper Alloy	38
29.	Microstructure of Martensitic Titanium-5.2pct. copper Alloy	39
30.	Microstructure of Quenched, Polished and Etched Titanium-8.0pct. copper Alloy	39
31.	Microstructure of Quenched, Polished, Etched and Aged(one day) Titanium-8.0 pct. copper Alloy	40
32.	Microstructure of Quenched, Polished, Etched and Aged(three days) Titanium-8.0 pct. copper Alloy	40
33.	Microstructure of Polished and Transformed (Martensitic) Titanium-43 pct. zirconium Alloy	41
34.	Microstructure of Polished and Transformed (Martensitic) Titanium-43 pct. zirconium Alloy	41
35.	Microstructure of the Titanium Martensite Needles	42
36.	Microstructure of the Titanium-1.5 pct. copper Martensite Needles	42
37.	Diagram Showing Morphology of Martensite in Titanium and Steel	64
38.	Microstructure of Mechanical Twinning in α Titanium	66
39.	Microstructure of α Titanium	66
40.	Microstructure of Quenched, Polished and Etched Titanium	67

INTRODUCTION

High strength to weight ratio and high corrosion resistance are often the main considerations that lead to the use of titanium base alloys. The mechanisms of phase transformation are among the fundamental properties upon which the response of the titanium base alloys to heat-treatment depends and considerable variation of mechanical properties can be produced by transformation of the high temperature β phase in titanium base alloys. Control of cooling rate, isothermal transformation, quenching and tempering determine the transformation structure and the properties. Previous studies on titanium base alloys with β stabilising elements[1] have shown that, on quenching from the β range the high temperature β solid solution (body-centered cubic) is not retained at room temperature unless the concentration of the alloying element is above a critical value. At lower concentrations it transforms, at least partially, into a supersaturated solid solution (close-packed hexagonal) designated "α'". The reaction is similar to the martensite transformation[2] in steels quenched from the γ field and is also termed "Martensite Transformation".

The temperature at which the martensite reaction takes place ("Ms") has been determined for several titanium binary alloys[3,4,5]. Holden et al.[6] in their work on the heat-treatment and mechanical properties of titanium-copper alloys constructed tentative Ms temperature vs. composition curve for alloys containing upto 5.2 pct.* copper.

---

* All compositions are atomic pct. unless otherwise stated.

In spite of the great amount of work done on martesite transformation in titanium base alloys, the martensite transformation temperature in pure titanium has remained doubtful. This is pricipally due to the difference in the purity of the metals used by the investigators and the difficulty in maintaining high purity during melting and heat-treatment. Similar difficulties have been noticed in the earlier work on high purity iron.

The present work is primarily concerned with the Ms temperatures in titanium - copper alloys containing upto 8 pct. copper.

Studies on the transformation in pure titanium , zirconium and iron have also been made to clarify the work done by earlier investigators and for purposes of comparision.

LITERATURE REVIEW

Earlier work on the titanium-copper system has been limited to the phase diagram determination by Joukainen et al.[7] and the effects of heat-treatment on mechanical properties reported by Holden et al.[6]. The phase diagram (Fig. 1) shows a eutectoid at 5.2 pct. copper and 798°C. The maximum solid solubility of copper in α titanium is reported to be 1.6 pct. copper at 798°C. The eutectoid reaction involves the decomposition of β to form α + Ti_2Cu. Holden reported that when Ti-Cu alloys in the eutectoid range are quenched from the β field, β transforms completely to α', which is generally considered to be a martensitic phase produced by a diffusionless reaction. No retained β was detected either by X-ray diffraction or microscopic studies. Holden constructed a tentative curve for Ms in Ti-Cu alloys plotted against composition up to 5.2 pct. copper (Fig. 1).

Many workers in the past have investigated the allotropic transformation in titanium[3, 8 to 15], zirconium[3, 16, 17] and iron[3, 18].

Allotropic transformation in titanium has been studied by McQuillan[8, 9, 10]. It consists of a change from the α (close-packed hexagonal structure) to high temperature β (body-centered cubic structure). The most recently reported value for the allotropic transformation temperature is 882.5°C[10]. The " equilibrium " temperature of transformation at which the free energies of the two phases are equal, is generally designated T_o (in iron this corresponds to the A_3 temperature). The allotropic transformation is sluggish in the vicini-

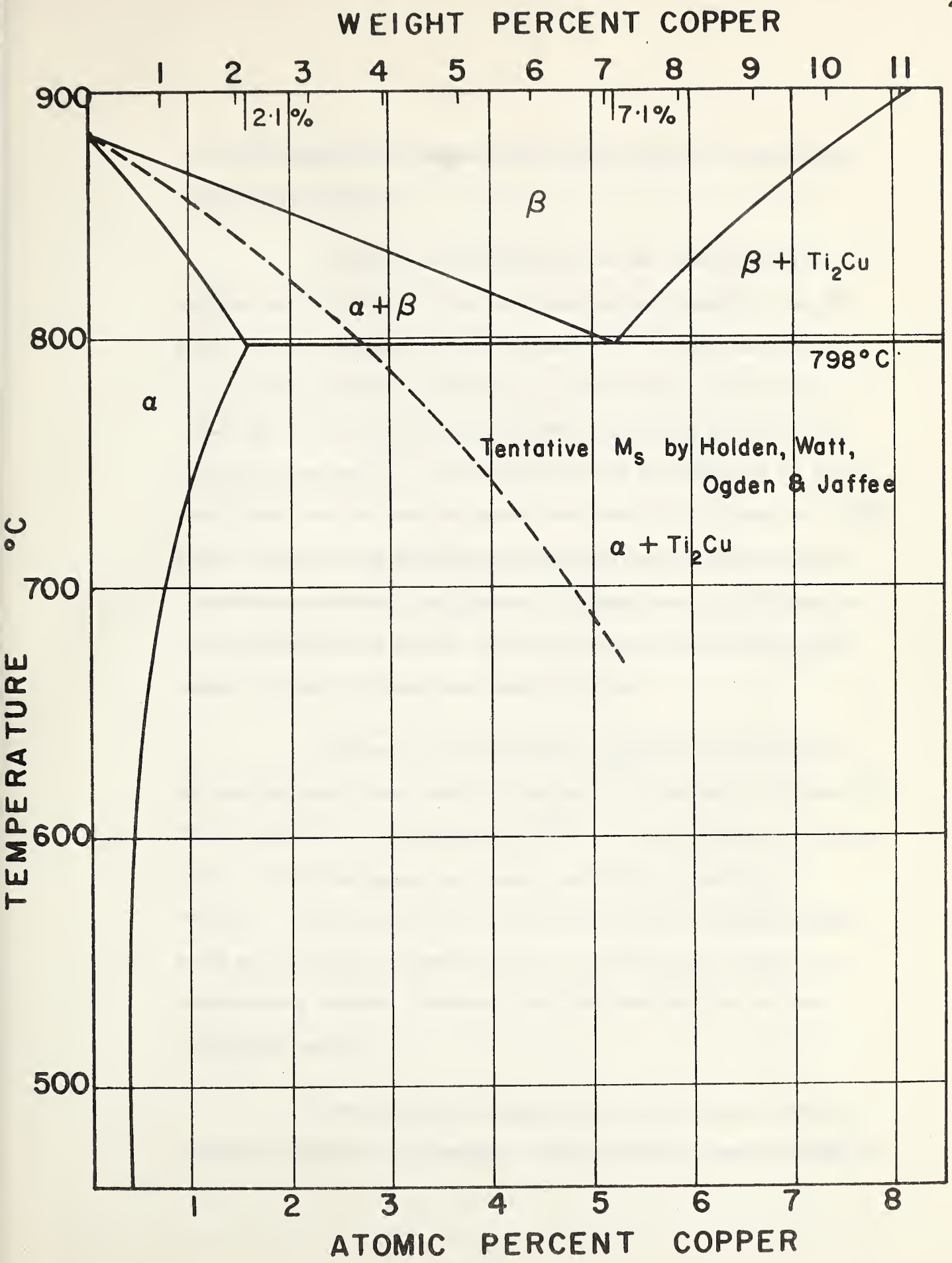

FIG 1

PARTIAL TITANIUM-COPPER PHASE DIAGRAM

ty of the equilibrium temperature, which indicates a nucleation and growth process.

The effect of cooling rate on the transformation temperature in titanium has been studied by Duwez[3]. The β phase in pure titanium cannot be retained at room temperature. On quenching from the β range a diffusionless, martensitic, $\beta \rightarrow \alpha$ transformation occers which has been evidenced by surface rumpling[11]. The transformation temperature on quenching titanium has been reported to be 850°C[3]. Wiskel et al.[12] in their work on the $\beta \rightarrow \alpha$ transformation reported that titanium transforms martensitically even at cooling rate of 2°C/minute at a temperature of 845°C. They also reported that there was about 0.01 pct. nitrogen and oxygen pickup.

Studies on crytallography of $\beta \rightarrow \alpha$ transformation in titanium have been made by Burger[13], Newkirk and Geisler[14], McHargue[15] and Williams et al.[11], and suggestions have been given for the homogeneous shear mechanism occuring in titanium. Williams et al. supplimented their crystallographic work on allotropic transformation in titanium by a number of microscopic studies. However this problem has not yet been completely solved.

Zirconium and titanium are very similar in their physical properties. Zirconium undergoes the same type $\alpha \rightleftharpoons \beta$

transformation at a transformation temperature of 865° C. Hayes and Kaufmann[16] studied the allotropic transformation in zirconium in 1953. However, no conclusion could be reached on the nature of the transformation. Gaunt and Christian[17] in their work on crystallography of $\beta \rightarrow \alpha$ transformation in zirconium demonstrated surface rumpling on polished surfaces. The surface rumpling was observed to be reversible above 500°C, indicating the transformation to be martensitic.

Although many studies have been published on phase transformations in iron base alloys, the early results of Esser et al.[18] and Duwez[3] seem to be the only ones obtained on high purity iron and at high rates of cooling. According to Esser the $\gamma \rightarrow \alpha$ transformation in relatively pure iron could be depressed from its " equilibrium " value of 905°C (A_3) to about 500° C at a cooling rate of 10,000°C/sec. The carbon content was reported to be less than .017 pct., but little was said about other impurities. Duwez reported a decrease in the transformation temperature from 905°C to 750°C at a cooling rate of 10,000°C/sec. The decrease in transformation temperature was much smaller than the decrease in $\gamma \rightarrow \alpha$ transformation temperature reported previously by Esser. The carbon content was less than .001 pct. The probable reason for the lack of agreement is stated to be in the purity of iron and the effect of the hydrogen atmosphere used in Esser's experiment. On the other hand,

in the iron-carbon system, extrapolation of Ms vs. carbon curve[19] to zero pct. carbon shows the Ms for pure iron to be 520°C, which very much supports the work of Esser.

EXPERIMENTAL

A. Apparatus

1. High Rate Quenching Unit

The first phase of the project was the design and construction of a high rate quenching apparatus, in which small specimens under vacuum could be quenched with a blast of high purity helium gas. A pressure of 10^{-5} millimeter of mercury or less was required to avoid specimen contamination at the soaking temperature of 1000^{0} C.

The essential features of such a unit are:

(a) a maintained vacuum at the start of the experiment.

(b) a means of heating the specimen to the desired temperature.

(c) a system to record the variation of temperature of the specimen.

(d) a quenching jet to give a range of cooling rates.

(e) the avoidance of all porous materials, such as ceramics, that might outgas with increase in temperature.

The gas quenching technique was used for the determination of transformation temperature of carbon steels during rapid cooling by Greninger[19] in 1942. Lately the same technique was used by Duwez for the study of some titanium binary systems[3, 4, 5 and 20]. Duwez used samples in which chromel-

alumel wires were placed between two sheet sections of the metal and the assembly was spot welded. In our experiment the intermediate forming operations (to produce sheet) were avoided, and consequently less opportunity arose for sample contamination.

The unit consisted of three main sections.

1. Vacuum unit.
2. Quenching unit.
3. Recording equipment.

Figs. 2, $3^{(a)}$, $3^{(b)}$& 4 show the details of the apparatus.

High vacuum in the system was obtained by a 2 inch M.C.F., 65 litres per second fractionating oil diffusion pump backed by a mechanical pump. An oil trap between the two pumps prevented mixing of diffusion pump and mechanical pump oils in case of power failure. A Philips cold cathode ionization gauge, type P.H.G. 90, connected to the base of the quenching enclosure, measured the pressure. The calibration of the instrument was checked with a " Balzer " hot cathode ionization gauge. A 1-1/2inch diameter cold trap was mounted on the diffusion pump with an " O " ring vacuum sealed joint to prevent any oil vapour from entering the quenching unit. On the top of the cold trap a 2 inch "Speedivalve" separated the quenching and the vacuum units.

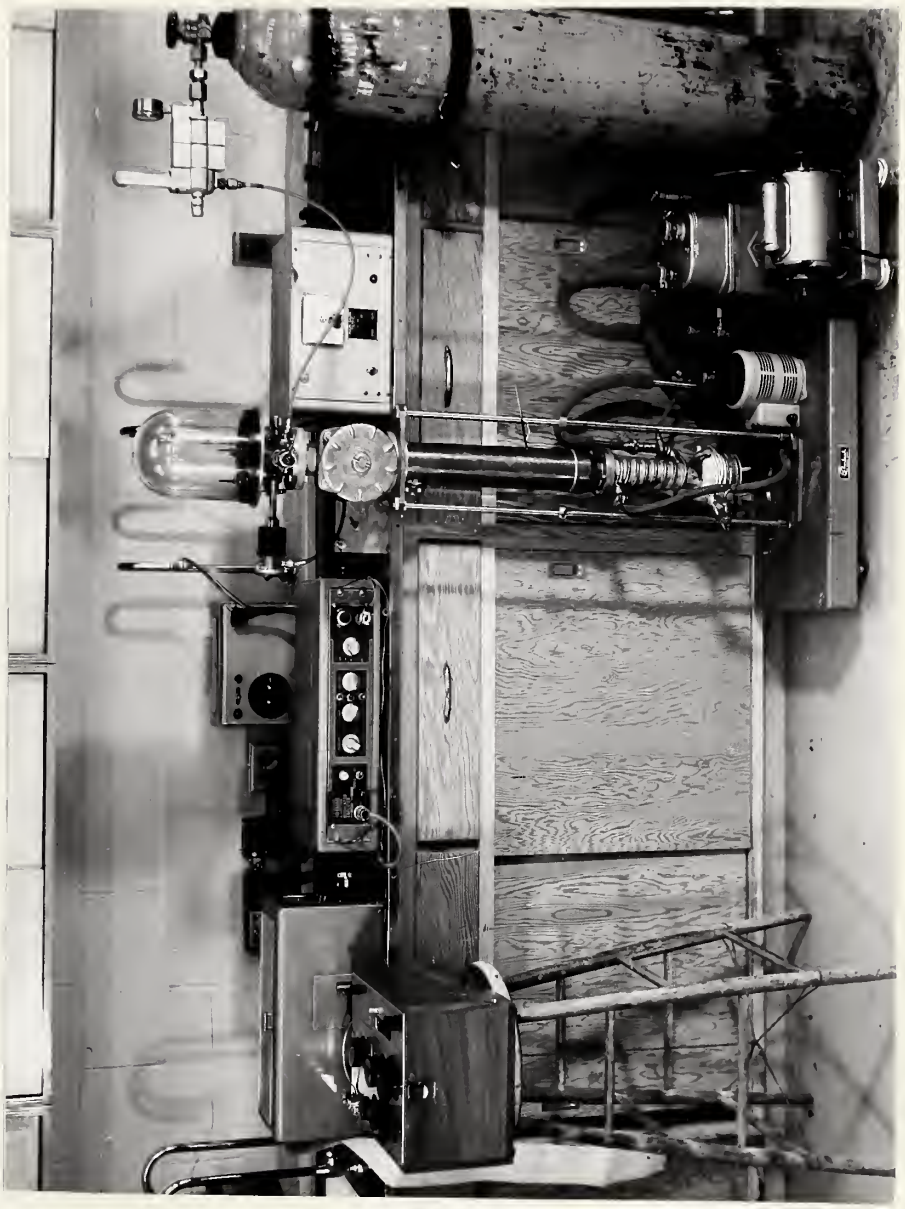

FIG. 2. APPARATUS ASSEMBLY

FIG. 3(a) QUENCHING UNIT

FIG. 3(b) THE HEATING COIL, QUENCHING JET AND THE SPECIMEN HOLDER ASSEMBLY

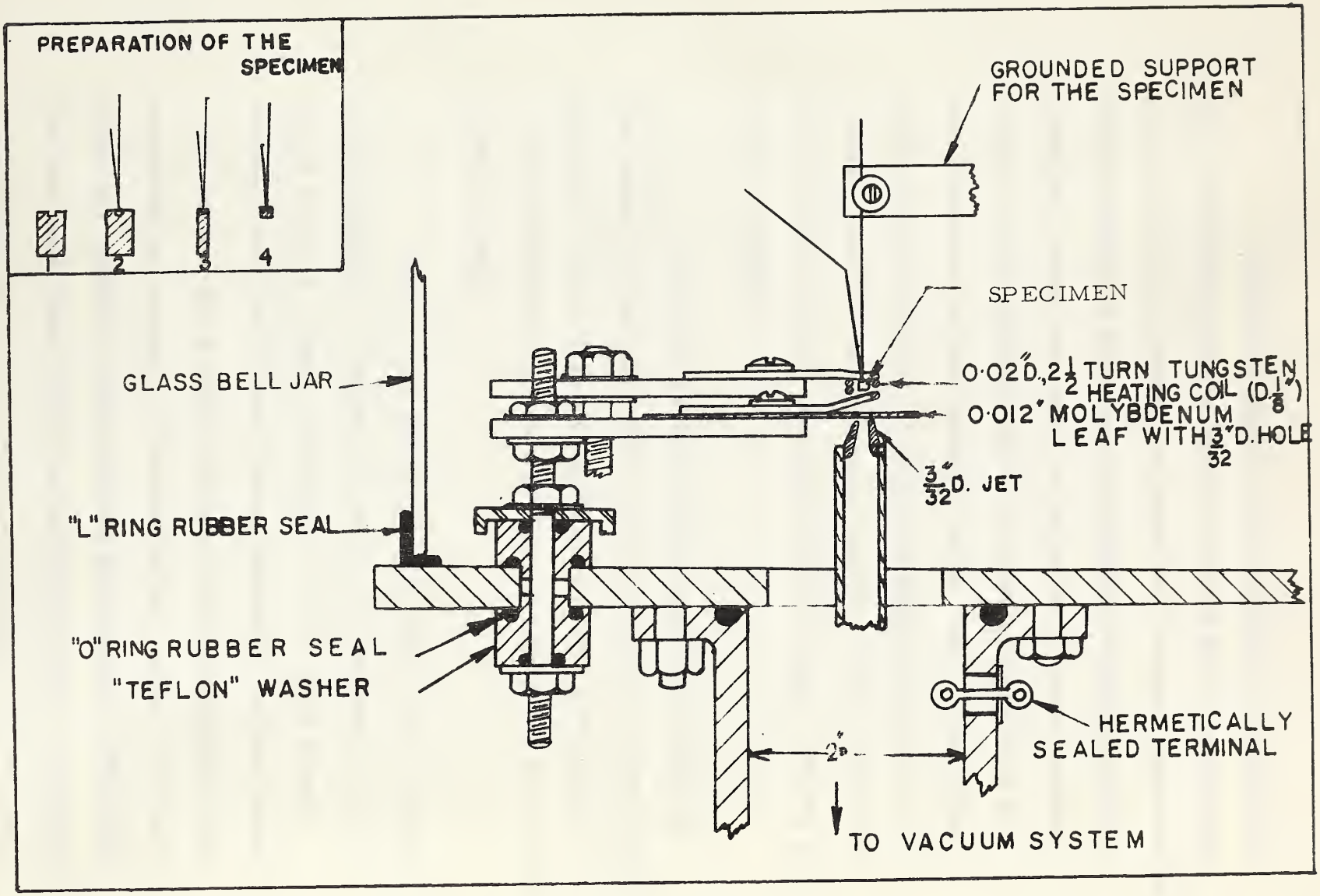

fig. 4 - CONSTRUCTIONAL DETAIL OF THE QUENCHING UNIT

The quenching unit was mounted on the speed valve. The auxiliary equipment was mounted on a 2 inch diameter and 2 inch long, flanged cylinder. Four vacuum sealed outlets on the cylindrical section were connected to the gauge, to a quenching valve, to a speed valve and to a vacuum release valve. Two hermetically sealed terminals on the same section introduced the thermocouple leads. The 7-1/4inch diameter flange contained a 1-3/4inch diameter hole at the centre which was the smallest cross-section in the vacuum line. A 2 inch high bracket, extending from the flange, held the specimen in position.

Two heavy current vacuum-sealed terminals on the flange provided the support and connection for a two and one half turn, 1/8inch diameter heating coil, which was made from .02 inch diameter tungsten wire fixed at a height of 1-1/4inches from the flange.

The coil was energised by a 300VA, 110V primary, 0-15V secondary, transformer, which in turn was in circuit with a Variac (3 amps, 0-140 V-S, 117-P). Slow rates of cooling (up to 200 ^{0}C/sec.) were obtained by uniform control of the Variac, via a drive with speed control tappings, at one revolution per second, 1/5 revolution per second, 1/60 revolution per second, 1/300 revolution per second, 1/900 revolution per second and 1/3600 revolution per second. Quenching was accomplished by control of high purity helium (99.999 pct.) blast via a quenching valve, operated externally.

A quenching jet, 3/32inch in diameter was fixed just below the coil. A molybdenum leaf, .012inch thick, with a 3/32inch diameter hole was arranged between the jet and the coil, to guard the jet against direct radiation from the coil. The jet, the leaf and the coil were fixed as close as possible without touching each other.

An inverted bell jar (diameter 6 inches, height 8-1/2inches) with a rubber " L " ring seal made the quenching enclosure.

The recorder used was an " Edin " multispeed magnetic oscillograph model 8082 operating in conjunction with EPSCO amplifier model 8108 A. The travel of the graph paper could be adjusted to 5, 10, 25, 100, 250 millimeters per second.

The leads from the thermocouple were connected via a two pole double throw toggle switch to potentiometer and recorder. The Pt-13 pct. (wt.) Rh lead was grounded throughout, while the platinum lead passed through and was insulated from grounded shields.

The potentiometer used was a " Tinsley " instrument, type 3184D reading to 10^{-3} m.v., without cold junction correction. The cold junction was at room temperature, with maximum variation of $\pm$ 1 ^{o}C during an individual run.

2. Specimen

The specimen (Fig.4) was a 3/64inch cube (approximately) attached to the end of the thermocouple. It was prepared in the following way: A hole, 1/32inch in diameter and 1/32 inch deep, was drilled in a sample of 1/8inch square cross section. The thermocouple bead was inserted and the sample squeezed and punched to hold the bead rigidly. The sample was then filed to a size of 3/64inch cube. The 0.012inch diameter thermocouple wires formed the support for the specimen. The specimen was cleaned in acetone and dried before it was put in the unit.

B. Experimental Method

Titanium-copper alloys were prepared from iodide titanium* and spectrographic standard copper* by levitation melting[21] in a high purity (99.999 pct.) argon atmosphere (Fig.5). The alloys were quickly heated above the melting point (where high frequency eddy currents insured a homogeneous alloy) and chill cast in split copper moulds. A weight check on the levitated samples showed a maximum loss of 0.08 pct. Metallographic examination of the samples showed uniform structure. Specimens were prepared from these levitated ingots in the way already described. The nominal compositions prepared were 0.5, 1.0, 1.5, 3.0, 5.2 and 8 pct. copper.

---

* See Appendix V for composition of the materials.

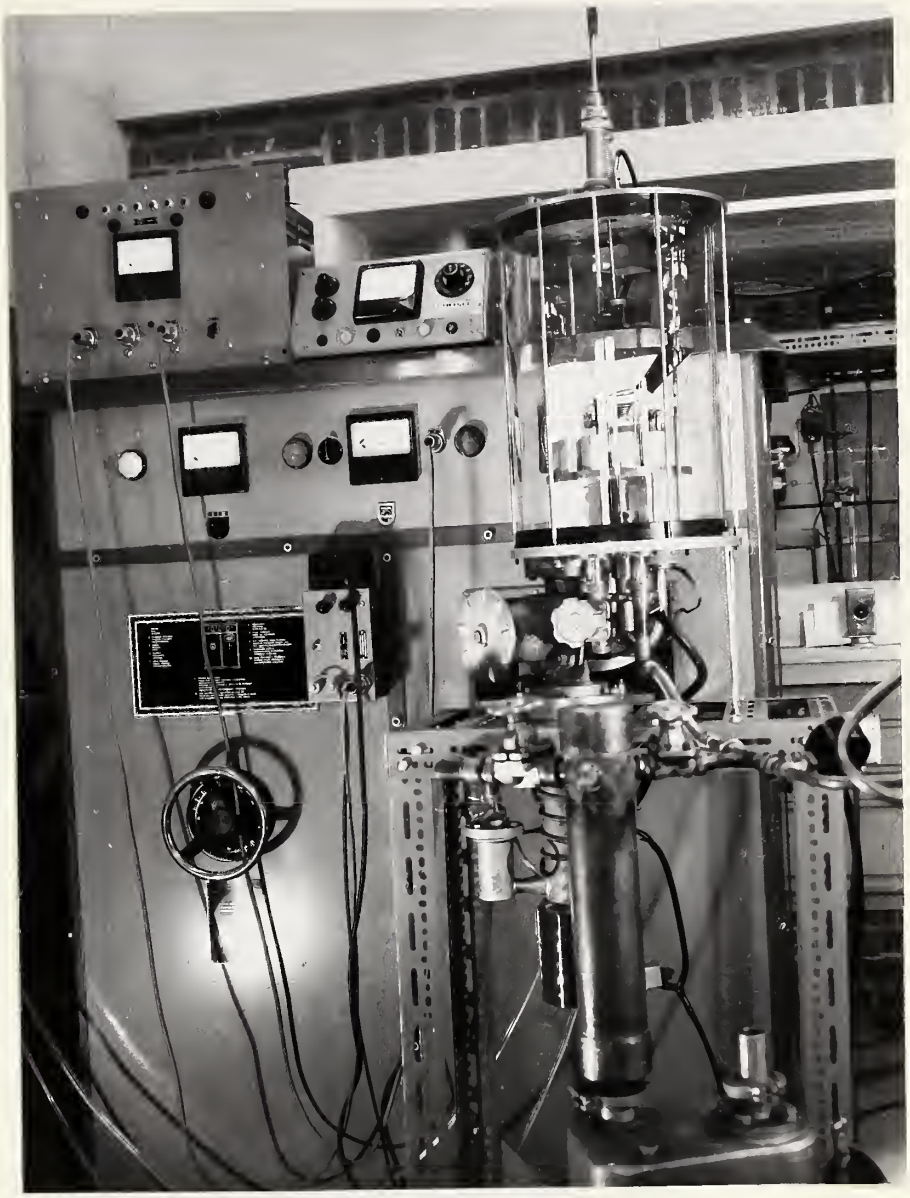

FIG. 5 . HIGH FREQUENCY LEVITATION UNIT

The quenching unit was outgassed under infrared heating for three to four days. Any new heating element was outgassed for four to five hours at a coil temperature of about 1400°C before the specimen was inserted. The pressure obtained was less than 5×10^{-7} millimeter of mercury at room temperature.

A positive gauge pressure was constantly maintained in the gas quenching tube. No decrease in the pressure could be observed after disconnecting the helium bottle, which demonstrated that the system was gas tight.

The specimen was slowly heated to 995 ± 5°C by manipulation of the Variac; the temperature was maintained for about 30 seconds and then the specimen was cooled or quenched. After each experiment the pressure was reduced to $< 10^{-5}$ millimeter of mercury before reheating prior to another quench on the same sample.

The amplifier was stabilized by switching it on one hour before use. The temperature scale of the recorder was calibrated against the potentiometer and it gave a straight line relationship. Repeated checks during the run showed negligible drift.

The nature of the cooling curves obtained is shown in Fig. 6. The transformation temperature is indicated by a break in the curve caused by the exothermic nature of the transformation. The transformation temperature was taken to be the start

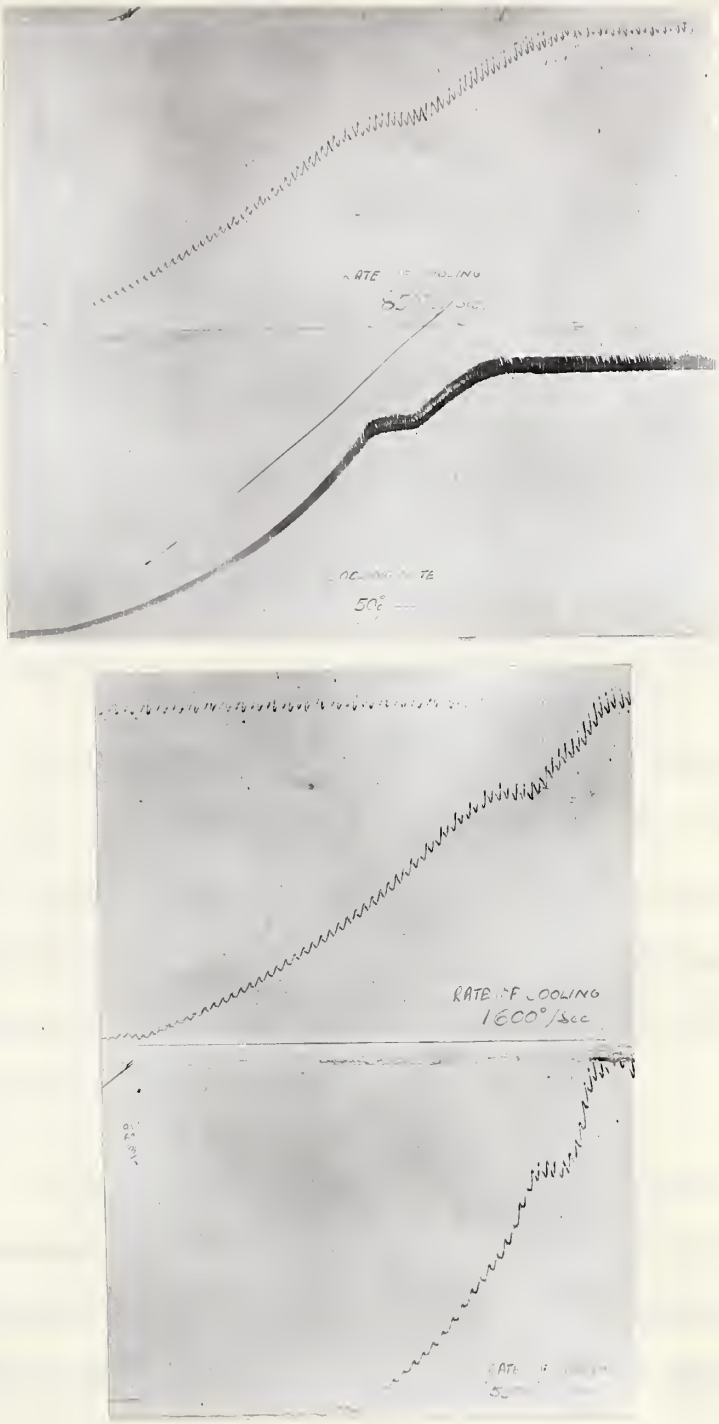

FIG. 6 . COOLING CURVES

of the arrest on the mean curve. Repetition with different samples of a given composition gave confirmatory results. The measured transformation temperatures are tabulated in Appendix I.

The break in the cooling curve could be located within one small division of the temperature scale on the graph (approximately 6°C). The room temperature variation was ± 1°C. These two errors combined give an error in the measurement of the transformation temperature of ± 4°C. With few exceptions, the measured transformation temperatures at high cooling rates in a given material lie within a band of 8°C.

A run was made with high purity iron* whose Ms temperature can be computed from available data[19]. The Ms temperature measured was 517°C, which is close to the calculated value of 520°C for pure iron. On slow cooling the transformation temperature was 912°C which compares well with the generally accepted A_3 temperature of 910°C.

A study was made on titanium ring samples (5/32 inch outer diameter, 5/64 inch inner diameter and 3/64 inch thick) to determine the effect (if any) of change of specimen shape on the transformation temperature. The results are given in Table 4.

---

* See Appendix V for composition.

A brief study was made of transformation temperatures on reheating the quenched specimens. The results are tabulated in Appendix II.

Metallographic samples of transformed materials were prepared by mounting the specimens in bakelite or in a steel clamp, polishing and etching with a solution containing 10 volumes of hydrofluoric acid, 10 volumes of nitric acid and 20 volumes of glycerine, followed by rinsing in 5 pct. nitric acid in ethyl alcohol. Further, many samples were mounted in steel clamps and polished prior to transforming, to reveal surface rumpling due to the martensitic transformation. The bright surface that remained after soaking at about 1000°C offered a reassurance of the cleanliness of the experimental technique.

Hardness of slowly cooled and martensitically transformed samples was measured in Vickers Pyramid Number (load 500 grams) on a Tukon tester and the results are given in Appendix III.

Electrochemical measurements were conducted on titanium and zirconium to evaluate the free energy differences between equiaxed and martensitic structures, both in the same metal. The results and the calculations of free energy differences are shown in Appendix IV.

RESULTS

A. Transformation Temperatures

The results on the measurement of transformation temperature Vs. cooling rate are shown in Fig. 7 to 9. In all the metals and alloys examined, the transformation temperature decreases as the cooling rate increases up to a certain critical cooling rate, beyond which the transformation temperature remains constant. The critical cooling rates for titanium, zirconium, titanium-zirconium alloy, titanium-copper alloys are shown in Table 1. Table 1 also shows their respective Ms temperatures. The determined Ms curve for titanium-copper alloys containing up to 5.2 pct. copper is shown in Fig. 10. The approximate Ms curve for the same composition reported by Holden et al.[6] has been included for comparison. The depression of the transformation temperatures below the corresponding equilibrium temperatures for titanium-copper alloys containing up to 5.2 pct. copper are presented in Fig. 11.

On reheating quenched samples of titanium, zirconium, titanium-zirconium alloy and titanium-copper alloys, the transformation to the high temperature β phase takes place at the temperatures shown in Table 1.

TABLE 1

Ms temperature , critical cooling rate and the transformation temperature on reheating quenched samples of titanium, zirconium, titanium-zirconium alloy and titanium-copper alloys.

Metals and Alloys	Ms °C	Critical cooling rate °C/sec.	Approx. transformation temp. on reheating quenched samples °C
Titanium (cube sample)	868	200	894
Titanium (ring sample)	863	400	894
Zirconium	860	300	868
Ti- 43 pct. Zr	497	60	500
Ti- 0.5 pct. Cu	857	200	873
Ti- 1.0 pct. Cu	842	150	874
Ti- 1.5 pct. Cu	827	120	835
Ti- 3.0 pct. Cu	745	120	796
Ti- 5.2 pct. Cu	625	900	795

B. Metallographic

The microstructures of slowly cooled (1-6°C/sec.) metals and alloys are presented in Figs. 13 to 20, 38 and 39.

Figs. 21 to 26, 28 and 33 to 36 show the polished and quenched structures of the metals and alloys. The quenched, polished and etched structures of a few samples are presented in Figs. 27, 29 to 32 and 40.

C. Hardness

The hardness values (V.P.N.) of slowly cooled and quenched samples of titanium-copper alloys are given in Table 15 and Fig. 12.

D. Electrochemical

Electrochemical potential measurements conducted on titanium and zirconium to evaluate the free energy differences between equiaxed and corresponding martensitic structures of the two metals implied values of 48 ± 10 cal/mol and 29 ± 5 cal/mol for titanium and zirconium respectively.

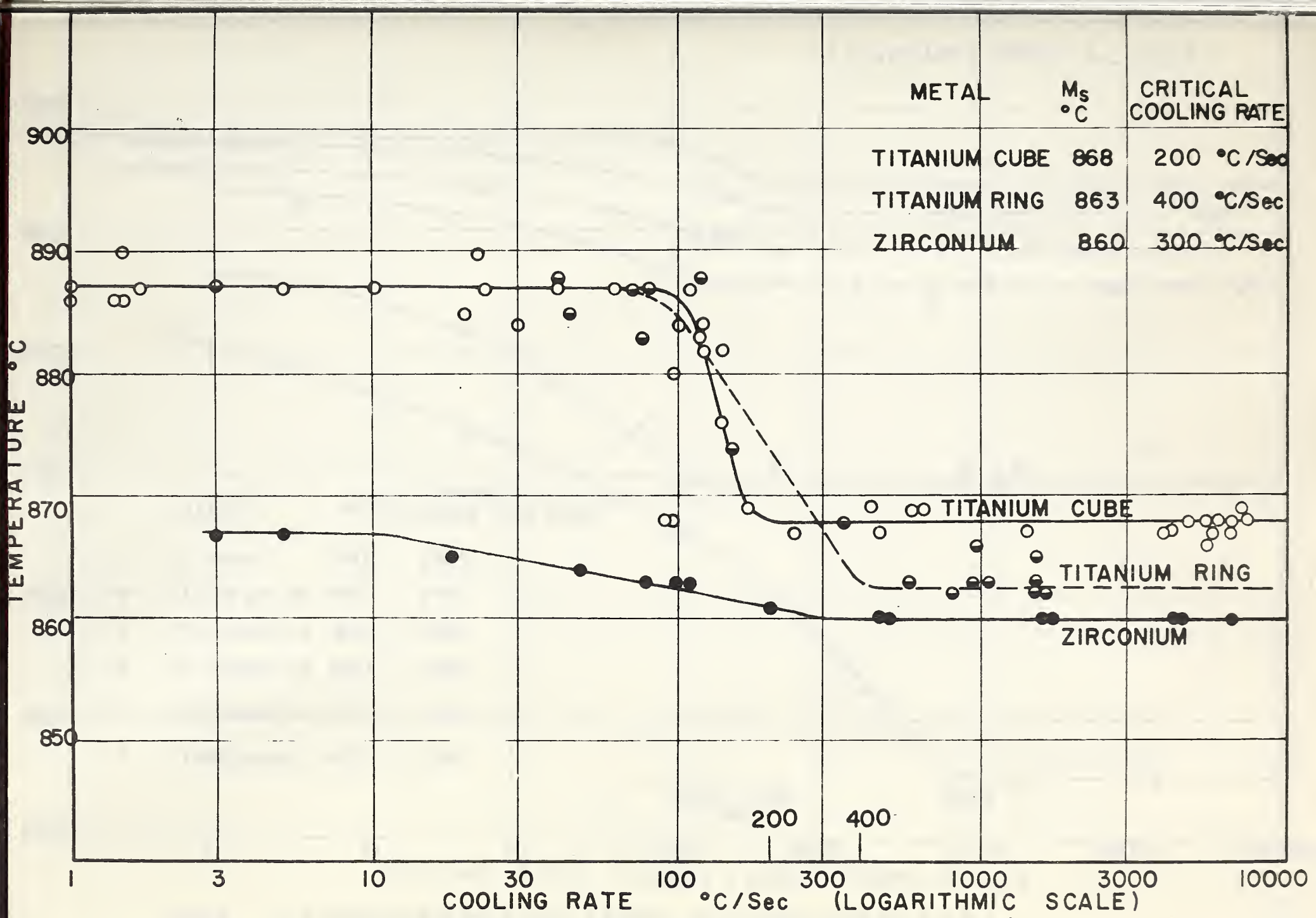

fig. 7 - TRANSFORMATION TEMP. Vs. COOLING RATE

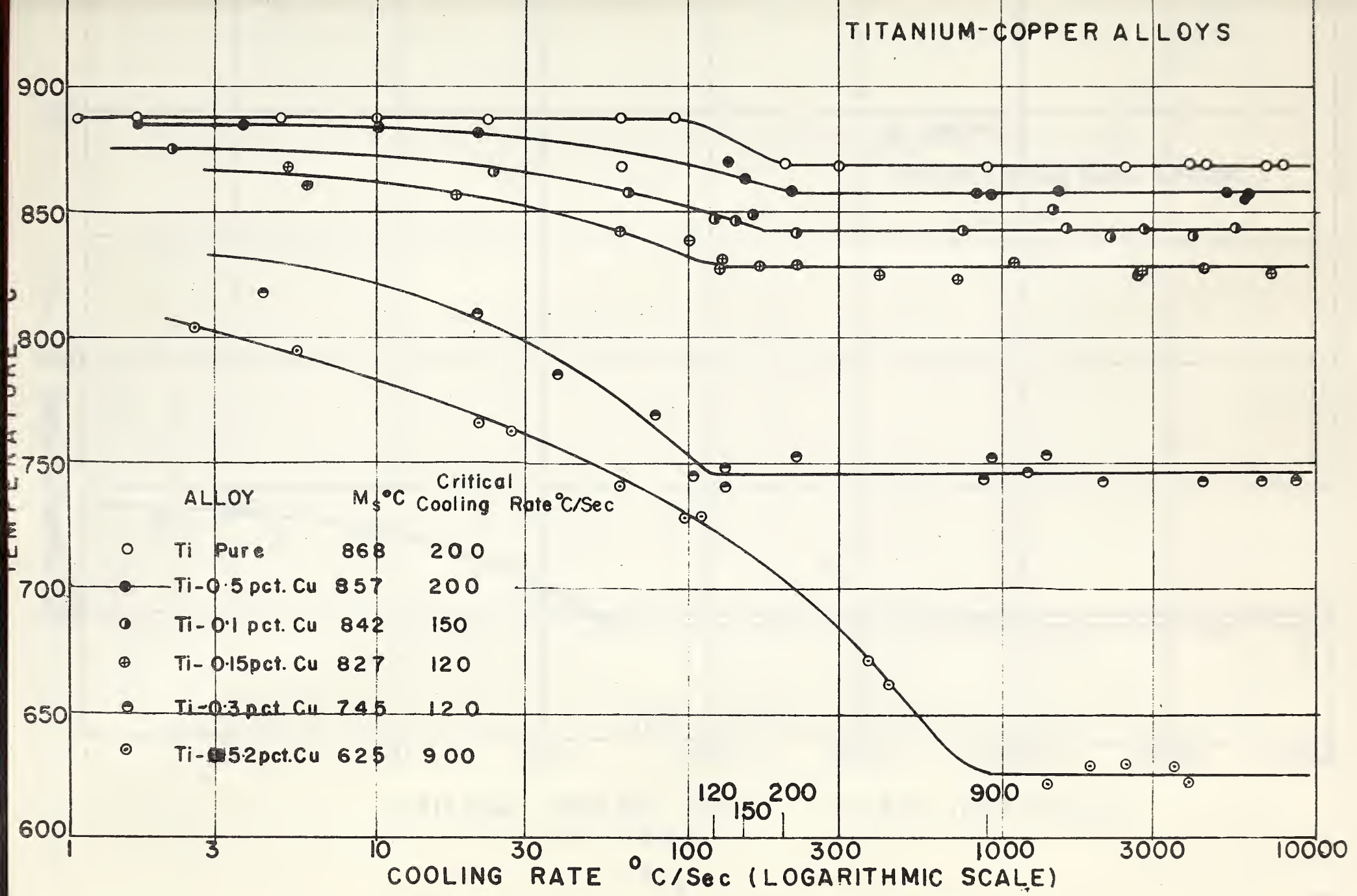

fig.8- TRANSFORMATION TEMP. Vs. COOLING RATE

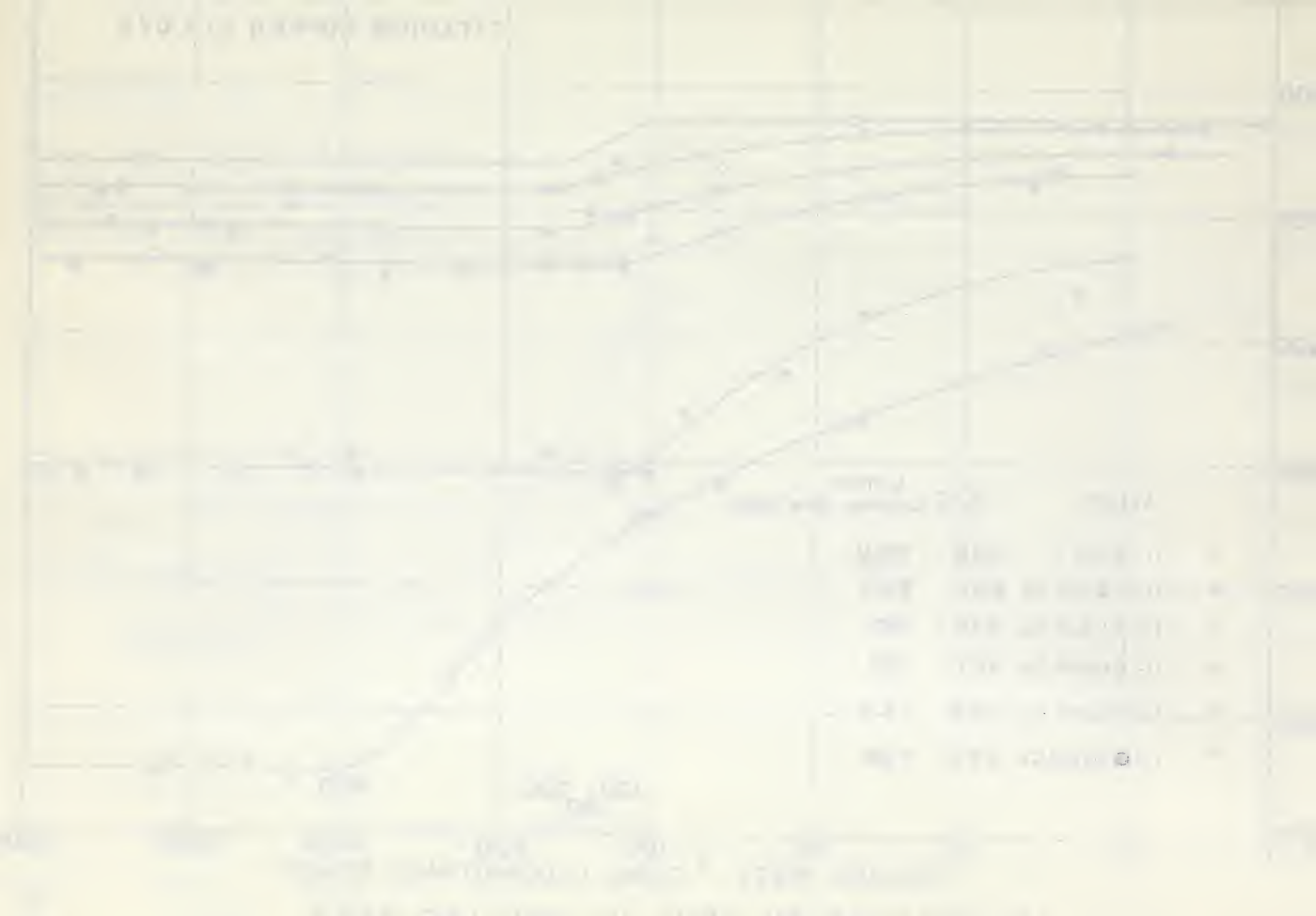

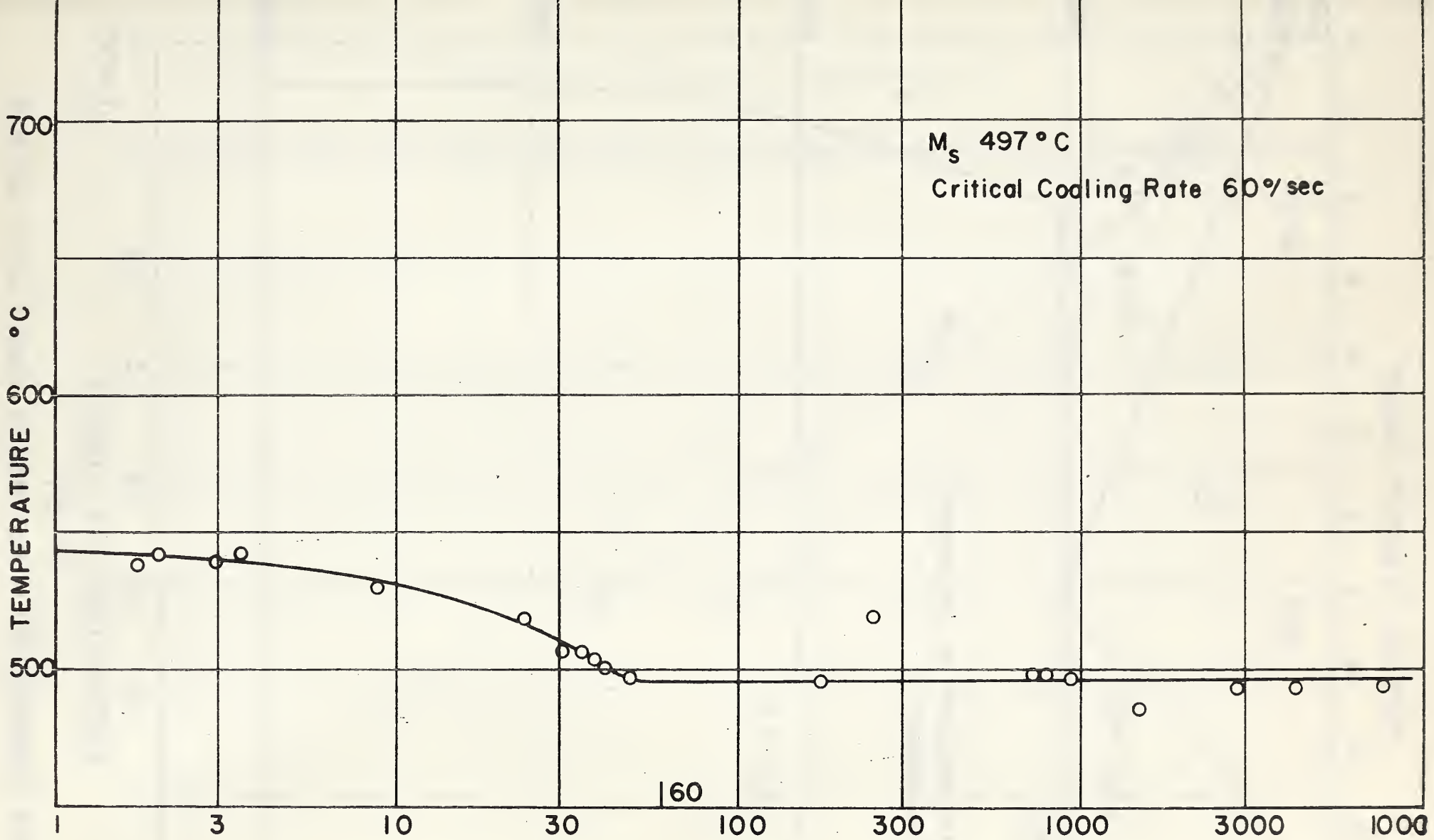

FIG 9

TRANSFORMATION TEMP. VS. COOLING RATE

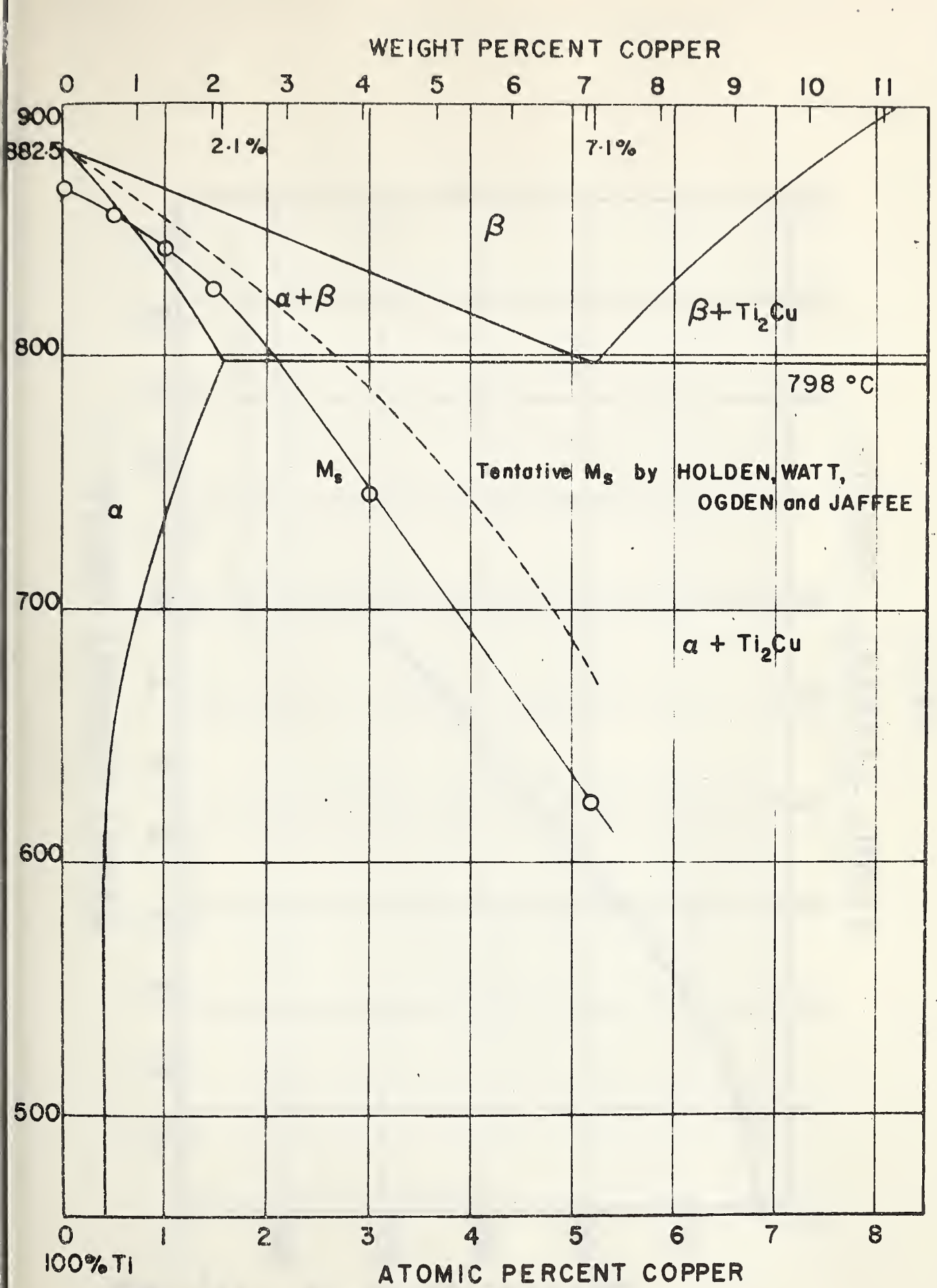

fig 10

PARTIAL Ti-Cu PHASE DIAGM. WITH DETERMINED Ms. CURVE

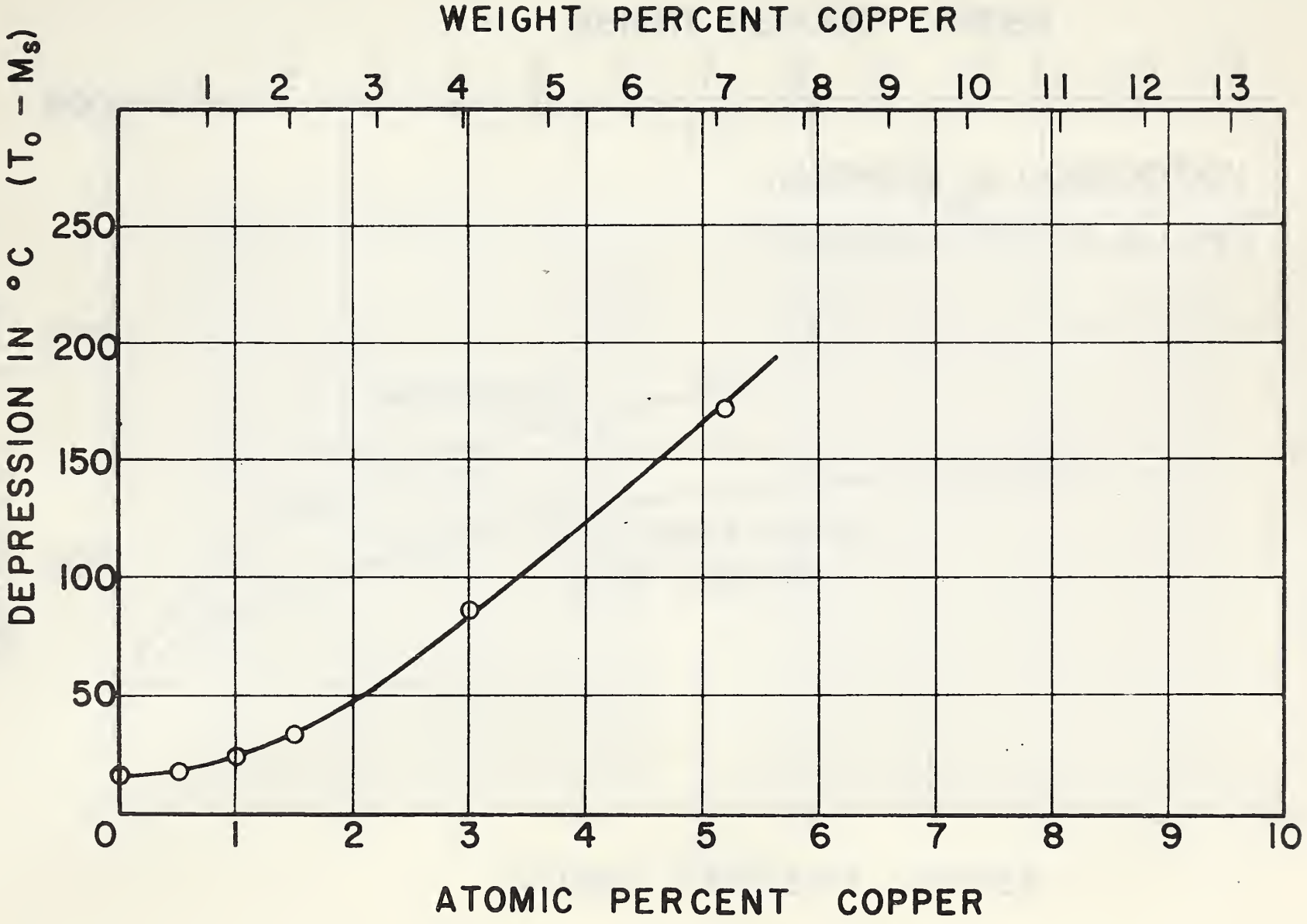

fig 11

DEPRESSION OF Ms BELOW THE EQUILIBRIUM TEMPERATURE IN Ti-Cu ALLOYS

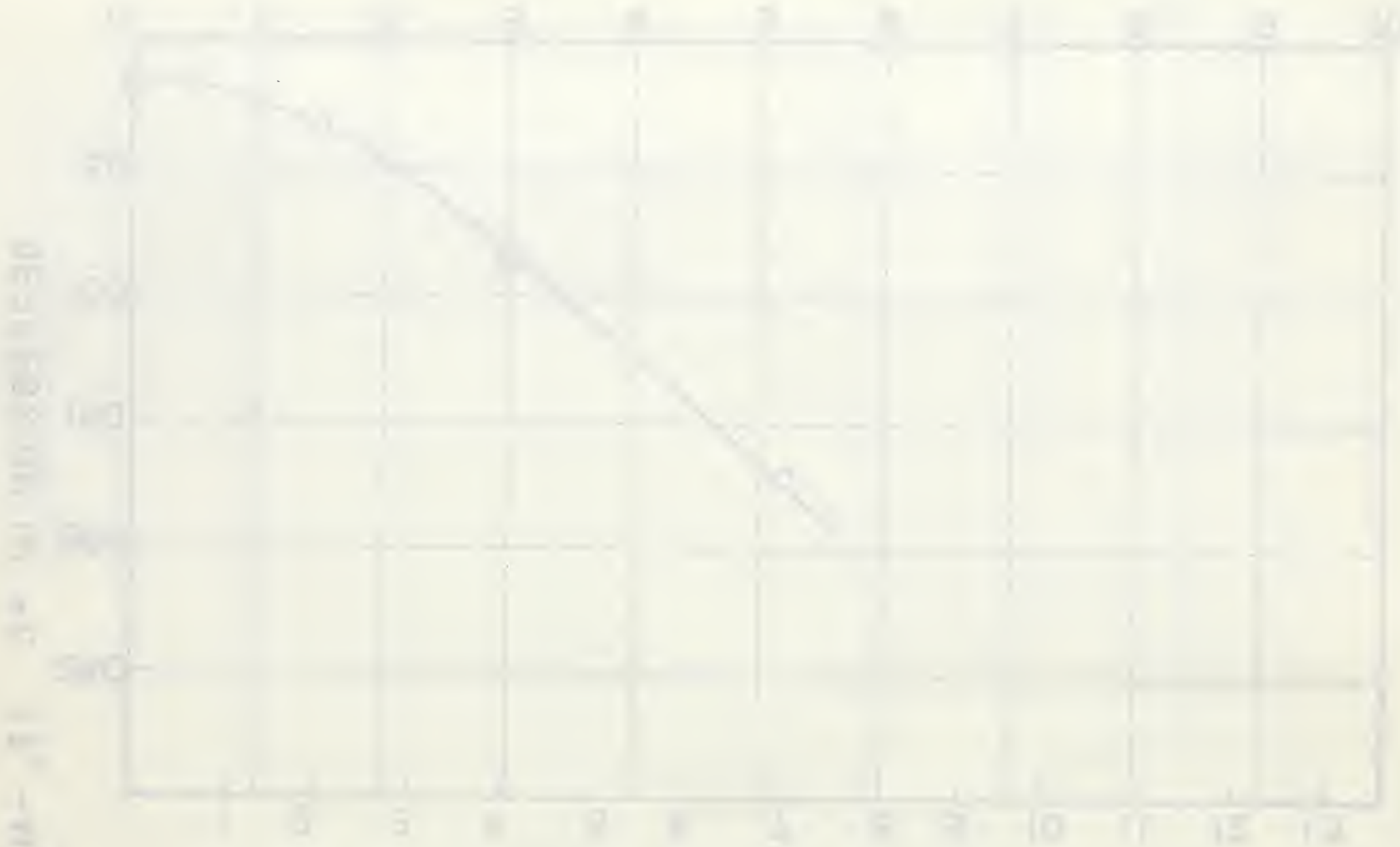

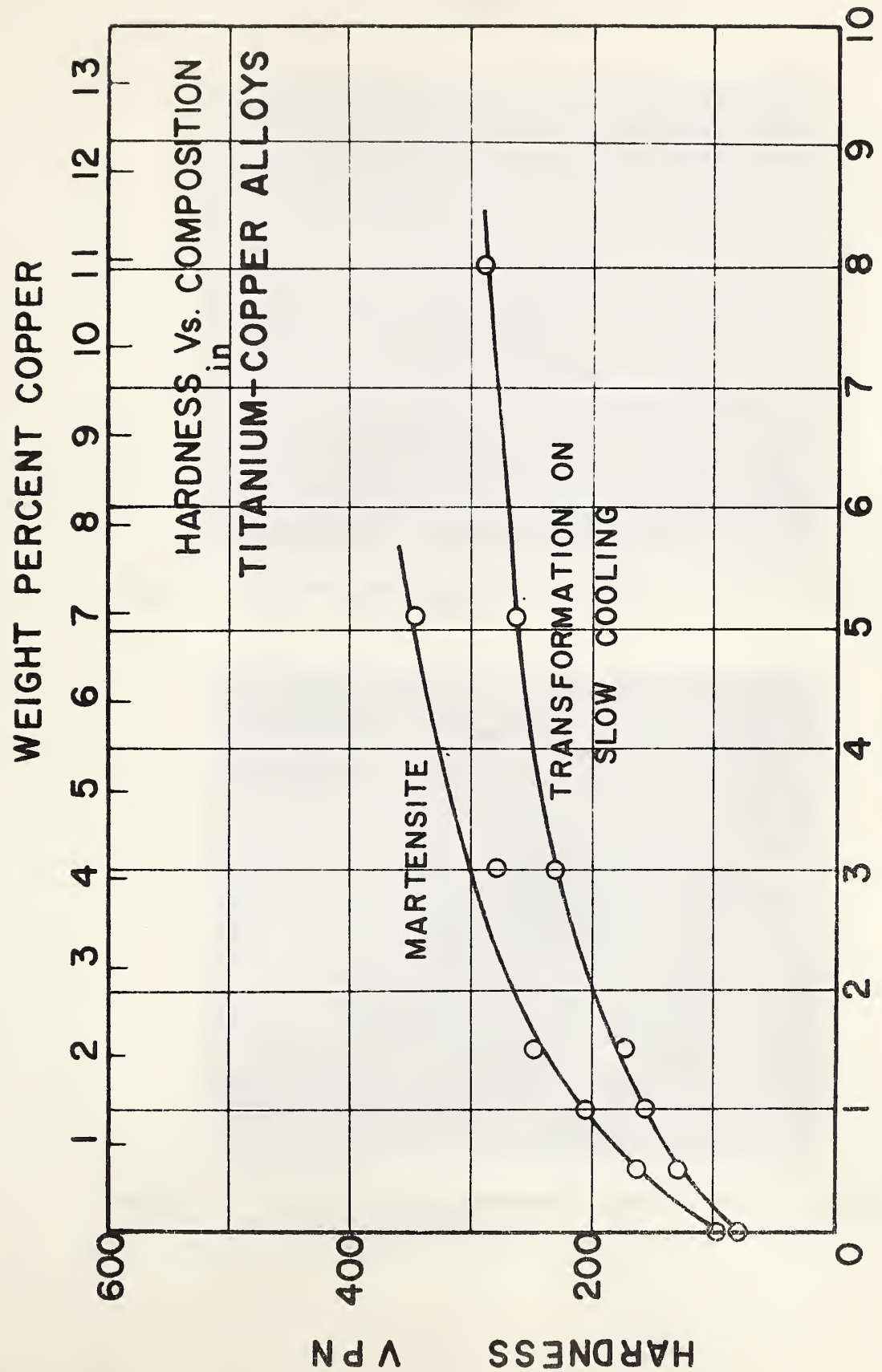
HARDNESS Vs. COMPOSITION in TITANIUM-COPPER ALLOYS
MARTENSITE
TRANSFORMATION ON SLOW COOLING
HARDNESS V P N
600
400
200
0
WEIGHT PERCENT COPPER
1 2 3 4 5 6 7 8 9 10 11 12 13
ATOMIC PERCENT COPPER
0 1 2 3 4 5 6 7 8 9 10

fig 12

MICROSTRUCTURES

Fig. 13 Polished and transformed (slowly cooled) iron x 150, (EQUIAXED)

Fig. 14 Polished and transformed (slowly cooled) titanium x 150, (EQUIAXED)

MICROSTRUCTURES

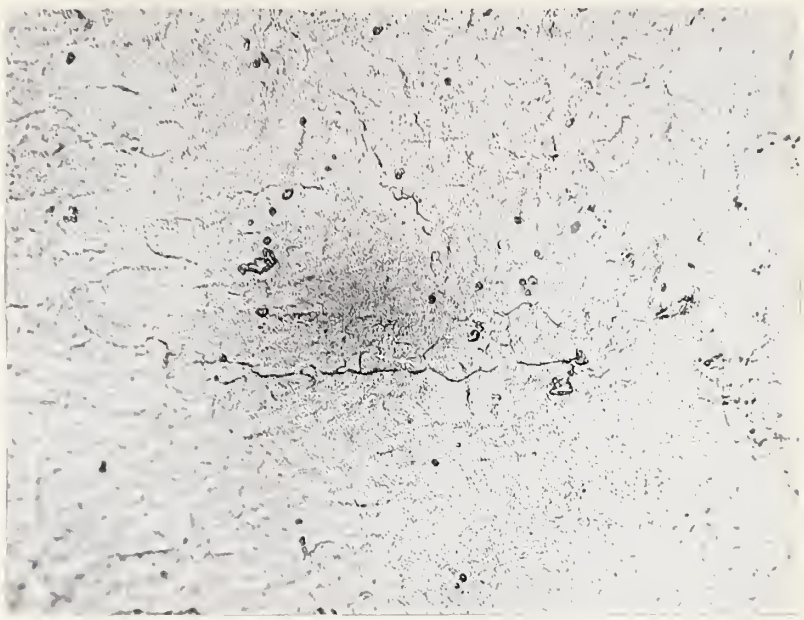

Fig. 15 Polished and transformed (slowly cooled) zirconium x 400

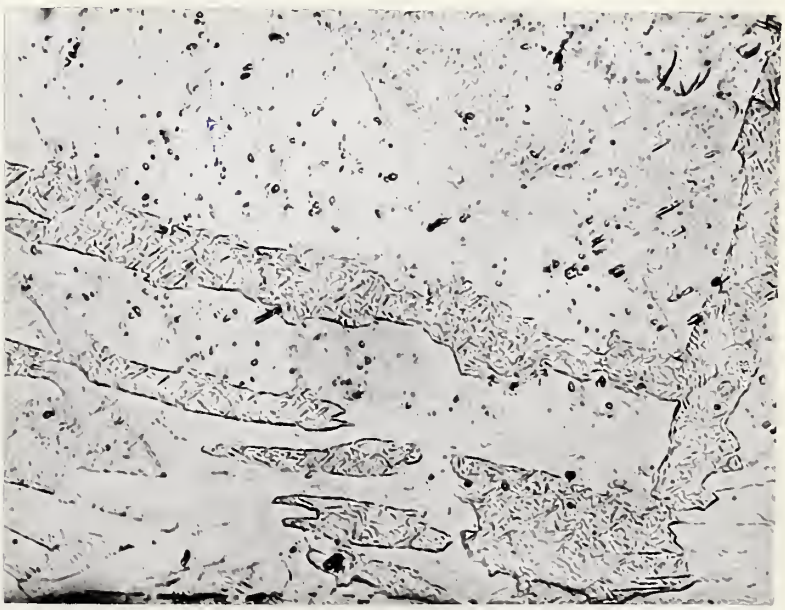

Fig. 16 Slowly cooled Ti-0.5 pct. Cu alloy x 450, etchant HF + HNO_3 + glycerine

MICROSTRUCTURES

Fig. 17. Polished and transformed (slowly cooled) Ti-1.5 pct. Cu alloy x 150

Fig. 18. Slowly cooled Ti-5.2 pct. Cu alloy x 300, etchant HF + HNO_3 + glycerine

MICROSTRUCTURES

Fig. 19 Slowly cooled Ti-8.0 pct. alloy x 300, etchant HF + HNO_3 + glycerine

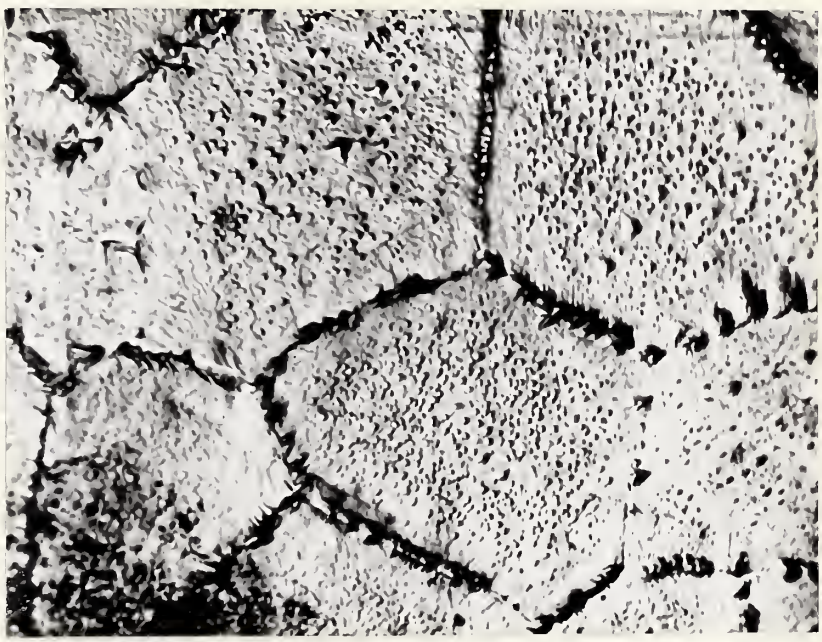

Fig. 20 Polished and transformed (slowly cooled) Ti-43 pct. Zr alloy x 350

MICROSTRUCTURES

Fig. 21 Polished and transformed (Martensitic) iron x 150

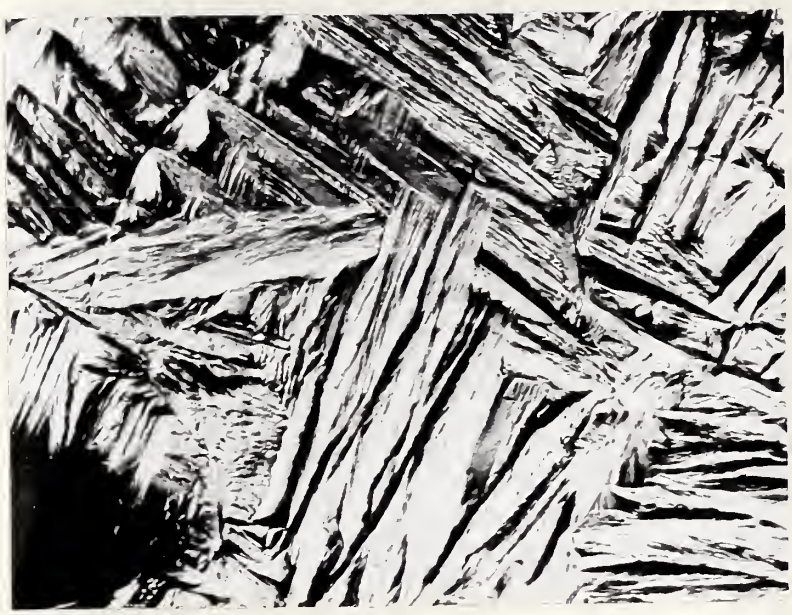

Fig. 22 Polished and transformed (Martensitic) titanium x 250

MICROSTRUCTURE

Fig. 23 Polished and transformed (Martensitic) titanium x 450, (twinned)

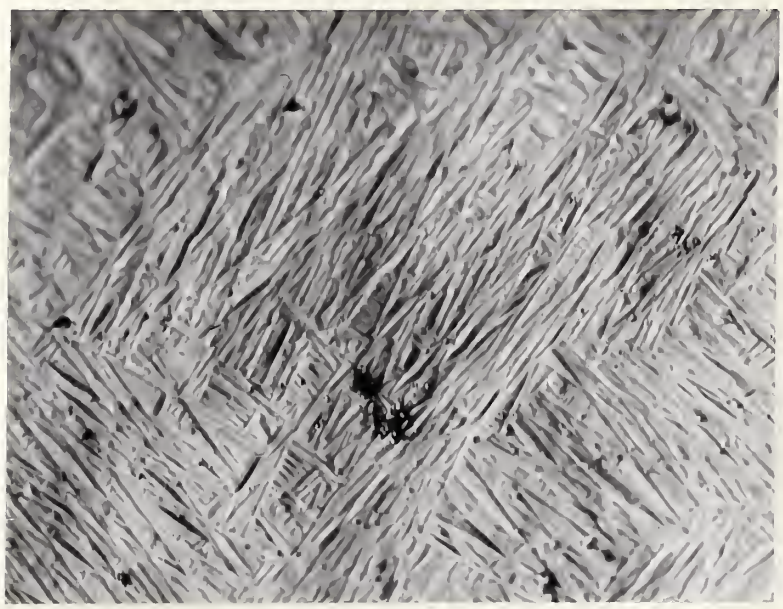

Fig. 24 Polished and transformed (Martensitic) titanium x 300

MICROSTRUCTURES

Fig. 25 Polished and transformed (Martensitic) Zirconium x 230

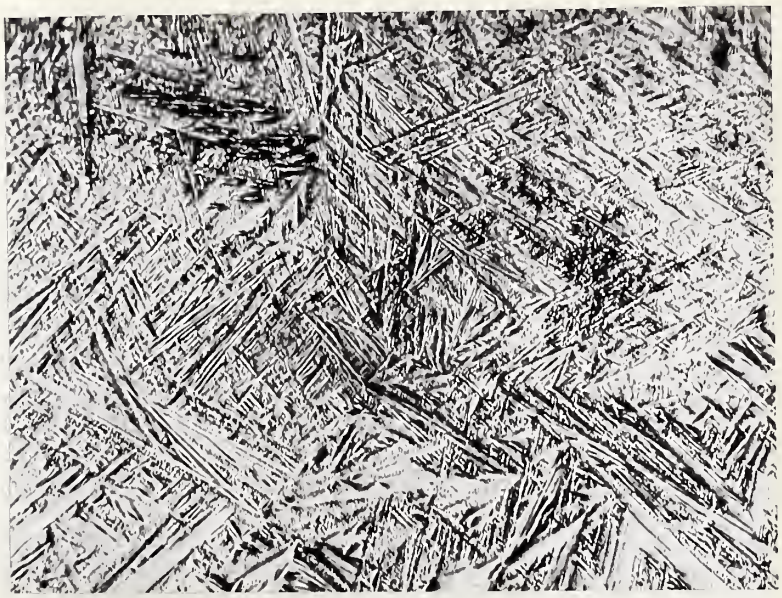

Fig. 26 Polished and transformed (Martensitic) Ti-0.5 Cu alloy, x 750

MICROSTRUCTURES

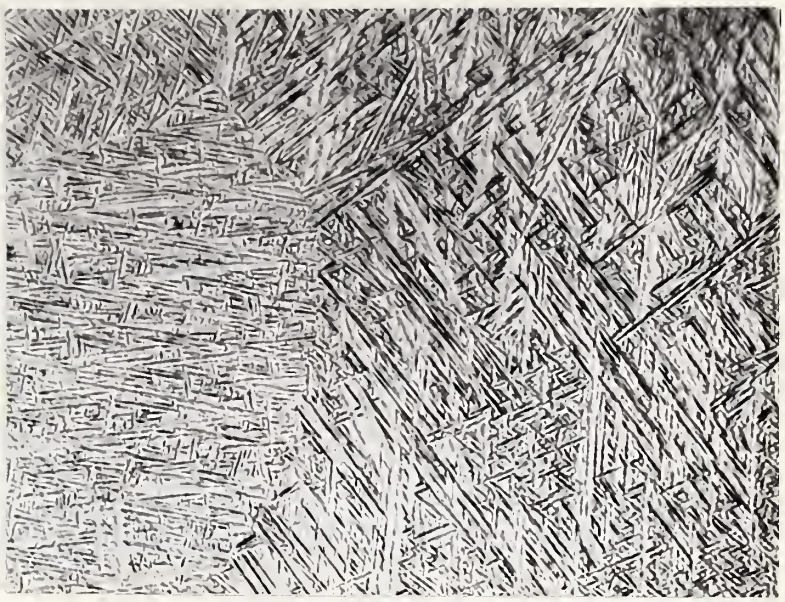

Fig. 27 Martensitic Ti-1.0 pct.Cu alloy
x 300, etchant HF + HNO_3 + glycerine

Fig. 28 Polished and transformed (Martensitic) Ti-5.2 pct. Cu alloy, x 200

MICROSTRUCTURES

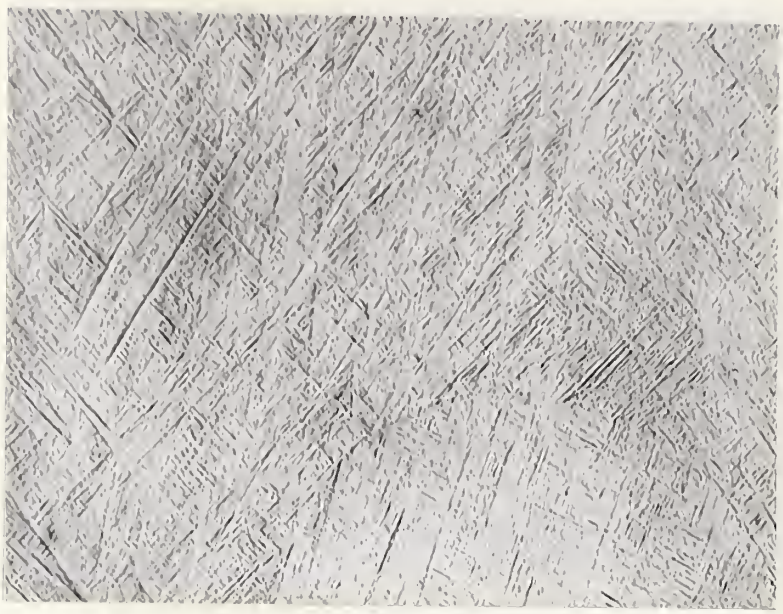

Fig. 29 Martensitic Ti-5.2 pct. Cu alloy x 300, etchant HF + HNO_3 + glycerine

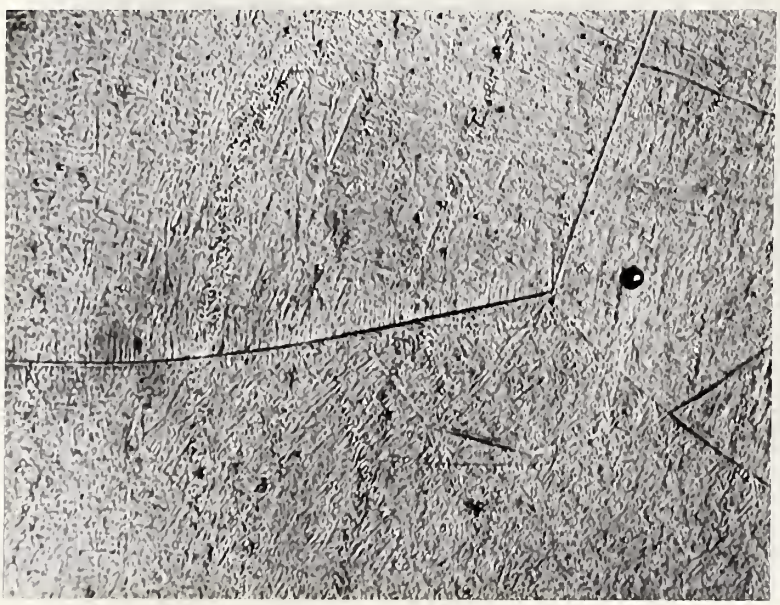

Fig. 30 Quenched, polished and etched Ti-8.0 pct. Cu alloy, x 750, etchant HF + HNO_3 + glycerine

MICROSTRUCTURES

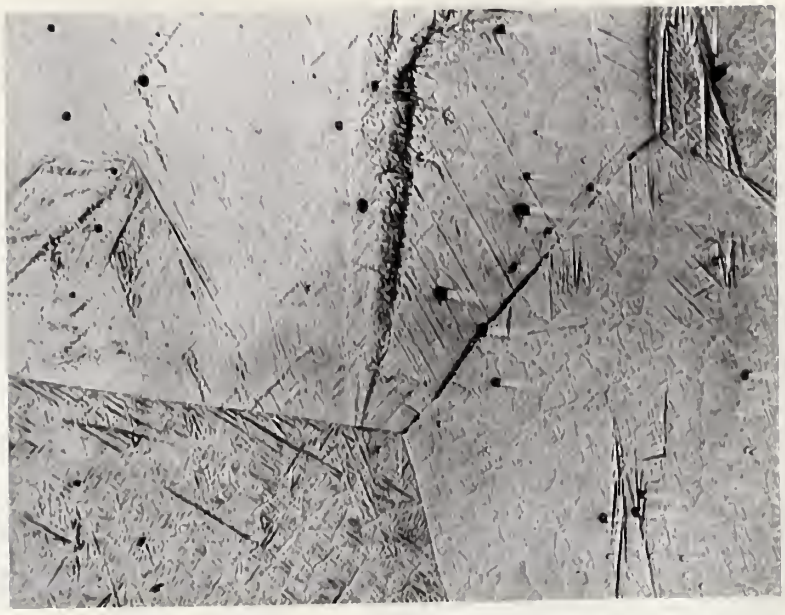

Fig. 31 Quenched, polished, etched and aged Ti-8.0 pct Cu alloy (substructure), x 750, etchant HF + HNO_3 + glycerine

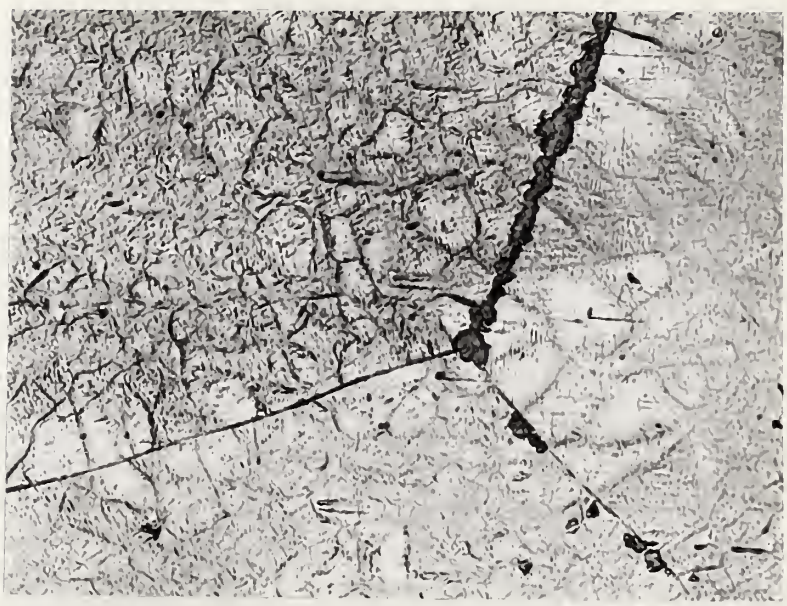

Fig. 32 Quenched polished, etched and aged (3 days) Ti-8.0 pct. Cu alloy , (pronounced substructure) x750, etchant HF + HNO_3 + glycerine

MICROSTRUCTURES

Fig. 33 Polished and transformed (Martensitic) Ti-43 pct. Zr alloy (cooling rate 150°C/sec.) x 100

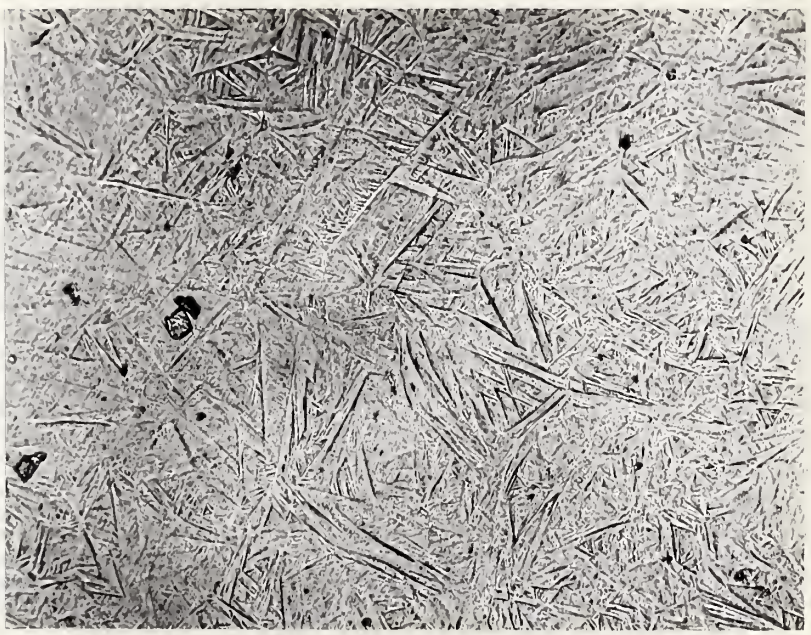

Fig. 34 Polished and transformed (Martensitic) Ti-43 pct. Zr alloy (cooling rate about 3000°C/sec.), x 150

MICROSTRUCTURES

Fig. 35 Titanium Martensite needles x 650

Fig. 36 Ti-1.5 pct. Cu Martensite needles x 1150

DISCUSSION

The discussion is given in three parts; first, a consideration of the results obtained on titanium-copper alloys; second, a brief appraisal of the results on titanium-zirconium alloy and third, a general discussion of the martensite transformation with particular reference to the pure metals, iron, zirconium and titanium.

A. Titanium-copper Alloys

The effect of cooling rate on the transformation temperatures in titanium-copper alloys is shown in Fig. 8. In all the alloys examined, there was a critical cooling rate beyond which no further depression in the transformation temperature was observed (except 8pct. copper alloy); this indicates that the transformation is most probably martensitic. This contention is supported by rumpling produced on polished and quenched surfaces of alloy samples. The rumpling is absent in slowly cooled samples. Microstructures showing martensitic and diffusion transformations are shown in Figs. 26 to 29 and 16 to 19.

The determined Ms curve is shown in Fig. 10 and the corresponding depressions in the transformation temperatures below the equilibrium are shown in Fig. 11. The Ms temperature decreases with increasing copper content up to 5.2 pct. copper. The decrease in Ms progressively increases with each additional amount of copper up to 2 pct. and assumes an almost straight li-

ne relation beyond 2 pct. copper.

The critical cooling rate derived from the curves (Fig. 8) decreases from 200°C/sec. for pure titanium to 120°C/sec. for the 3 pct. copper alloy and increases to 900°C/sec. at the eutectoidal composition of 5.2 pct. copper.

Observations on the 5.2 pct. and 8 pct. copper alloys show a different nature of transformation for hyper-eutectoid compositions. The increased critical cooling rate of 900°C/sec. in a 5.2 pct. alloy appears to be due to appearance of Ti_2Cu in the eutectoid and hyper-eutectoid compositions. Ti_2Cu seems to act as an active nuclei for the growth of diffusion products. The high temperature of transformation will be another factor for higher rates of diffusion and these could be sufficient to initiate the nucleation and growth process (diffusion) at even relatively higher cooling rates.

In the 8 pct. copper alloy, the transformation temperature was continuously depressed from 865 to 747°C as the cooling rate rose from 3°C/sec. to 200°C/sec. On rapidly quenching the behaviour was very irregular and in most of the quenches no transformation temperature was observed. A polished and transformed surface did not show rumpling and a quenched, polished and etched structure showed sharp grain boundaries. A finely distributed structure was observed within the grains (Fig. 30). The sample developed subgrains on aging at room temperature (Fig. 31). After three days of aging the sample had developed a

pronounced substructure with a precipitate at the grain boundaries (Fig. 32). A similar substructure[22] was observed in the retained β phase of Ti-Ni alloys by Polonis and Parr. X-ray diffraction studies on the sample showed lines corresponding to a close-packed hexagonal structure. Three lines, which could not be indexed in the pattern were believed to be due to Platinum—Pt-Rh thermocouple bead at the core of the specimen. However, exact calculations are difficult unless the composition of the bead is known.

The possible explanation for the substructure observed in 8 pct. alloy on holding at room temperature could be sought in, firstly the process of polygonisation[22] and secondly the " Aging ".

The mechanism of polygonisation is believed to occur by a process of vacancy diffusion[24] which only occurs at relatively higher temperatures where self diffusion is rapid. This decreases very much the possibility of polygonisation to occur on holding at room temperature. At the same time the boundaries in the observed structure appear to widen; get diffused and the structure as a whole darkens along with the subgrain boundaries. This indicates the possibility of appearance of some different phase rather than simply formation of a dislocation grain boundary and this suggests the occurence of the second process, i.e. " Aging ". At present it is only possible to guess that the new phase appearing could be Ti_2Cu. However, a Debye-Scherrer picture has failed to confirm such a small quantity of Ti_2Cu.

Gomez et al.[25] in their work on decomposition kinetics of α' in Ti-5.2 pct. copper alloy reported two different reactions occur during tempering of α'. One reaction involves relatively rapid decomposition of α' at the former β grain boundaries while the other reaction involves precipitation within the β grains. The 8 pct. alloy presents a similar situation occuring at a lower temperature and requiring a longer time.

The additional β grain boundaries in the 8 pct. alloy observed during aging could have resulted through unrelieved stresses set up during $\alpha \rightarrow \beta$ transformation on heating. Since Ti_2Cu is also present, the reaction on heating is $\alpha + Ti_2Cu \rightarrow \beta$. In hyper-eutectoid Ti-Cu alloys the $\alpha \rightarrow \beta$ reaction on rapid heating may proceed before Ti_2Cu decomposes and if the $\alpha \rightarrow \beta$ reaction is rapid, strains could be introduced in the grains, which will lead to polygonisation during soaking of β and will produce additional sub-boundaries. These boundaries may not be distinguished in a freshly quenched and etched sample (Fig. 30). In such a polygonised β phase (a fine network of grain-boundaries), the high irregularity in the atomic arrangement at the grain boundaries will act as barrier to the propogation of martensite plates and will result in a fine martensitic structure which may not be resolved under an ordinary microscope.

As a result of the martensite reaction, the atomic irregularity at the existing β grain boundaries will be even more distorted due to the additional strains set up by the arrest of martensite plates and the boundaries will become zones of high energy. The precipitation of low energy compounds can easily occur at such grain boundaries with an extremely fast nucleation and growth process at so called tempering temperatures. However, such local precipitation could occur slowly even at room temperature taking a much longer time to complete.

The additional darkening of the matrix as a whole (Fig. 32) may also occur by the second precipitation reaction reported by Gomez et al.[25].

Many favourable sites for nucleation exist within the transformed β due to the extremely large interfacial area associated with martensite plates. These interfaces could be the new sites for further precipitation of the compound after it has proceeded to some extent at the existing grain boundaries. However, these processes may not last very long at room temperature and the precipitation may remain incomplete.

Hardness measurements on a freshly quenched sample (362 V.P.N.) and on an aged sample showed an increase of 3 hardness points. This may be a negligible change in hardness*, but it might be associated with the small amount of precipitate observed (Fig. 32).

---

* a change of about 10 points would be considered significant.

Hardness measurements on slowly cooled samples of titanium-copper alloys containing up to 8 pct. copper showed increasing hardness with copper content ranging from 78 V.P.N. for pure titanium to 289 V.P.N. for the 8 pct. copper alloy (Fig. 12). The rate of increase of hardness declines with increasing copper content; beyond 5.2 pct. copper, the increase is small.

The hardness of martensitic samples rises more sharply with composition than the hardness curve for slowly cooled alloys. The difference in the two hardnesses of the same alloy progressively increases from 16 V.P.N. in titanium to 85 V.P.N. in 5.2 pct. copper alloy. In a substitutional type of alloy, like Ti-Cu, the increased hardness of martensite compared to the hardness of a slowly cooled structure in the same alloy is associated with the strains within the martensite transformation.

B. Ti-Zr Alloy

A titanium-zirconium alloy of " pseudo-eutectoid " composition (Ti-50 pct. Zr) was selected to study its behaviour in comparison to the constituents titanium and zirconium. This alloy is a single phase solid solution of titanium and zirconium in the β as well as in the α phase and the transformation occurs at a specific temperature ($545^{\circ}C$)[20] —not over a temperature range . This alloy might be expected to behave similarly to the pure metals titanium and zirconium. Unfortunately, due to experimental errors, the alloy which was prepa-

red analysed 43 pct. Zr and the comparison could not be attempted.

Studies on the titanium-43 pct. zirconium alloy gave an Ms of 497°C (Fig. 9) and a critical cooling rate of 60°C/sec.

A sample cooled slowly (4°C/sec) from the β field showed the transformation to occur by a diffusion process (Fig. 20), but the same sample cooled at higher rates of cooling (higher than the critical cooling rate) transformed martensitically. Figs. 33 and 34 show the martensite structure developed on polished surfaces of specimens cooled at rates of 150°C/sec. and about 3000°C/sec. respectively. Microscopic examination of the specimen cooled at 150°C/sec. and then polished and etched showed a partially transformed martensitic structure. It appears that some β phase has been retained by increased rate of cooling.

Duwez[20] in his work on " Allotropic Transformation in Titanium-Zirconium Alloys " reported noticeable retained β solid solution in alloys containing 10 pct. of either titanium or zirconium and the amount increased progressively with addition of one metal to the other. The Ms temperature for titanium -43 pct. zirconium alloy obtained from his Ms curve is 500°C.In these respects, the results of the present work on titanium- 43 pct. zirconium alloy agree with the previously reported work by Duwez.

C. Martensite Transformation

A substantial amount of research[26 to 28, 3 to 5] has been conducted on the occurence of martensite in steels, in other iron alloys, in non-ferrous alloys of Cu-Al, Cu-Zn, Cu-Sn, Li-Mg, Ti-Fe, Ti-Ni, Ti-Zr, Ti-Mn, Ti-Cr, Ti-Mo, Cobalt-binary alloys and in the pure metals Fe, Co, Ti, Zr and Li to determine the characteristics, the kinetics and the cystallography of the transformation. The martensite transformation generally has the following features;

1. The transformation is diffusionless and involves no change in chemical composition.

2. The transformation involves shear and the most convenient experimental feature to use in order to identify a reaction as martensitic is the characteristic change of shape revealed on a flat surface by the tilting of the regions transformed.

3. The transformation on cooling starts after undercooling below the equilibrium temperature T_o at a temperature Ms. While most of the martensitic transformations in steels and non-ferrous alloys have been studied under " athermal " conditions, " isothermal " martensites[29 to 37] have been observed in several cases, both with and without prior " athermal " transformation. While some workers believe that isothermal transformation is suppressible under rapid cooling, another school of thought insists that the martensitic transformation is at all times isothermal;

if this is suppressed by very rapid cooling, the high temperature phase will persist at the temperature of the quenching medium.

4. The Ms temperature is uniquely determined by the chemical composition of the material and usually is lowered with increasing solute content (except in steels containing Co and Al).

5. The transformation may occur smoothly or in sudden " bursts"[38] in which a large amount of martensite is suddenly formed and the reaction is completed in a fraction of a second.

6. The martensite transformation in some systems has been shown to be reversible during heating.

7. The transformation proceeds with formation of new plates rather than growth of pre-existing plates.

8. An individual martensite plate usually forms in a very short time, even at low temperatures, but exceptions have been found in Au-Cd[39], In-Th[40, 41, 42], Mn-Cu[43], U-Cr[33] and Aluminium Bronze[44] in which slow growth of martensite has been observed.

9. Martensite forms coherently with the parent phase and various crystallographic relationships[26, 27, 45] have been given for the processes occuring in different metals and alloys.

10. Higher hardness is observed in martensitically transformed

steels and many other alloy systems. However, it is not an essential characteristic of a martensite transformation.

11. The kinetics of transformation are significantly altered by:
    (a) interrupted cooling.
    (b) applied stress.

12. Martensite is a metastable phase between the parent and the final equilibrium phase, although it may persist for an indefinite period at room temperature.

While crystallographic studies on the transformation have produced fairly consistent results, there is much conflict in the proposed theories for the mechanism of the transformation.

The two groups of mechanistic theories that predominate are by Fisher et al.[28, 46, 47, 48] and by Cohen et al.[28, 49, 50, 51]. They both suggest the natural nucleation and growth type of process for martensite formation, but differ in the nature of the embryo from which the martensite originates.

The classical nucleation and growth theory has been extended to the formation of martensite by Kurdjumov[53] and his associates and by Fisher, Hollomon and Turnbull. As martensite appears to be coherent with the parent austenite, the nucleation theory is modified to include the effects of plastic distortion. Fisher et al. dealing with iron-carbon martensites suggest that martensite nucleates from embryos of carbon free austenite regions in an otherwise structurally perfect austenite of average concentration. Their precise model

of the nucleus visualizes that these carbon free austenite regions contain within them a small ferrite region just large enough to nucleate ferrite in the carbon free austenite upon quenching. However, no carbon free austenite regions have been detected.

Cohen et al. consider that the martensite transformation is brought about by nucleation at " strain embryos " and subsequent propogation of a shear wave over a " reaction path ". This path is described by the relative motion of the atoms during the transformation. They further believe in the existence of a free energy barrier opposing propogation. When the embryo surmounts this barrier the transformation proceeds instantaneously, even at subzero temperatures and cannot be suppressed by rapid quenching. The theory differentiates between the " athermal " and " isothermal " transformations and suggests that the transformations occur by different mechanisms.

The isothermal martensite transformation has been observed in alloys of Fe-C-Mn[34, 35], Cu-Al-Mn-Ni[44], Cu-Sn[44], U-Cr[33], Fe-Ni-Mn[34, 37], Fe-Ni[31], Fe-Cr-Ni steels[32] and other steels[29, 30] which necessitated consideration of an " isothermal " mode of martensite transformation. Kurdjumov[53] and Crussard[54] both believe that there is no athermal martensite transformation but only an isothermal one. Kurdjumov believes that such a transformation originates from homogeneous classical nucleation at preferred sites due to thermal fluctuations at the temperature of transformation. However, he does not define the nature of the embryo. A similar theory has been proposed by Philibert and Crussard, who suggest that the transforma-

tion occur by random classical nucleation caused by thermal fluctuations and that all the martensite transformations occur in isothermal increments. The athermal nucleation is a manifestation of extremely rapid isothermal nucleation. Crussard calculated the rate of isothermal nucleation on the basis of the Boltzmann probability equation and suggested that the rate of nucleation is so high that it justifies the invariance of Ms with cooling rate. The high rate of cooling for martensite transformation is only required to suppress the diffusion transformation. This theory seems to take into account a number of characteristics of martensite transformation. However, a few characteristics which still need explanations are:

1. Holding in the austenite range depresses the Ms temperature on further cooling.

2. Martensite transformation occurs by a plate by plate process and does not nucleate throughout the mass simultaneously as would occur in homogeneous nucleation.

3. A thermoelastic equilibrium between original and martensitic phases was observed by Kurdjumov[44, 54].

The crux of martensite formation today appears to be less concerned with the origin of the nuclei (this is in any event an extremely difficult matter to determine experimentally). Rather it is concerned with the question of whether martensite propogation occurs isothermally or athermally.

The concept of driving force

On the basis of nucleation theories and the concept of critical embryo size, it was possible to calculate the amount of free energy needed to start the martensite transformation[50]. This is defined as the " driving force " of the martensite reaction. One may also predict the Ms temperature. However, a number of assumptions are made in the calculation which remain questionable;

1. The data which is based on a system in equilibrium is employed in calculations for a non-equilibrium system. The concept of " driving force " implies that there is a free energy difference between austenite and martensite at the Ms, while in the calculations the criterion for Ms is that the free energies (of the two phases) are equal.
2. The assumption that the free energy difference (F_A-F_M) represents not only a driving force but also an activation barrier appears to be quite unsatisfactory.
3. Data on the Fe-C system [47] gives an extrapolated Ms of 520°C for pure iron; but from the Fe-Ni system [55] the extrapolation gives an Ms of 650°C.

4. The activation barrier is a common phenomenon in a classical nucleation and growth (diffusion) type of transformation. The driving force could reasonably be expected to arise from surface and strain energies only. That is (T_o - Ms) for iron and iron binary alloys (taking surface + strain energy to be $\sim$ 65 cal/mol[28]) should be of the order of 50°C; but the observed values are more than 200°C.

The following discussion does not propose a new theory of the martensite transformation but attempts are made to clarify a few of the differences observed in the martensite transformation in pure iron, titanium and zirconium.

The results of measurements on pure titanium are summarized in Fig. 7. The scatter between the transformation temperatures measured lies well within $\pm$ 4°C. which is the estimated accuracy of measurement. The transformation temperature is observed to be constant beyond a certain rate of cooling. This indicates that the transformation at these rates is martensitic at 868°C - a fact which is confirmed by microscopic evidence (Fig. 22 to 24). The surface rumpling on a titanium sample cooled at 300°C/sec. appeared very much more twinned than the characteristic martensitic structure (Fig. 23). The depression of the transformation temperature is 15°C below the equilibrium temperature of 882.5°C[10] and the estimated critical cooling rate is 200°C/sec. (Fig. 7).

The Ms temperature (850°C) reported by Duwez[3] appears to be quite low in comparison with the result of this inves-

tigation. The possible reason for the difference could be in the purity of the metal used. This is substantiated by the result of Wiskel et al.[12], who reported Ms for a contaminated sample of titanium (approximately 0.01 pct. oxygen and nitrogen) to be 845°C.

It is observed (Fig. 7) that the transformation temperature is further depressed by 5°C when the sample is changed from a 3/64 inch cube to a 5/32 inch ring. This depression may not be significant in consideration of the experimental error ± 4°C, but it appears that there is some effect of the stress system involved in the martensite transformation in a ring sample. The difference in the shape of the ring sample leads to different temperature gradients and hence different thermal stresses across the sample. These, in turn, may affect the transformation temperature, because of the influence these stresses will have upon the dilatometric stresses of the martensite transformation. At present and in the view of the small temperature difference between Ms measured in the ring sample and the cubic sample, a quantitative appraisal would be presumptuous. However, the external stresses have been shown to have significant effect[56-61] on Ms temperature.

On reheating quenched samples of titanium a transformation occurs at a temperature of 894°C. This temperature differs slightly from the transformation temperature(886-890°C)obtained on reheathing a slowly cooled sample(The equilibrium temperature of $\alpha \rightleftharpoons \beta$ transformation temperature obtained on reheating quenched samples). In view of mar-

tensite reaction and its reversal in Fe-Ni[62], Fe-Mn[57], Cu-Zn[59], Cu-Al[63,64], Cu-Sn[59], Li-Mg[65], metals cobalt[66], Zr[13], and Li[65], it is possible that martensite in titanium reverses to a high temperature β phase at 894^{0}C. However, this could not be confirmed with the existing apparatus.

Theoretical calculations on the titanium-zirconium system made by Kaufmann[67] showed the driving force of the martensite reaction in titanium-base dilute alloy to be $\sim$ 40 cal/mol. This in turn implies that the Ms temperatures of dilute titanium base alloys and of titanium will lie about 40^{o}C. below the corresponding equilibrium temperatures. In this respect the value reported by Duwez[3] and Wiskel et al.[12] seems to be nearer to the calculated value. But Kaufmann's calculation is based on a doubtful principle of applying equilibrium thermodynamics to a non-equilibrium system. At the same time the thermodynamic parameters of titanium and zirconium determined by earlier workers have differed greatly and it is difficult to select the best values.

Because zirconium and titanium have very similar physical properties it was anticipated that the effect of cooling rate on transformation in zirconium would be similar to that in titanium. However, zirconium on cooling showed a depression in the transformation temperature of 7^{o}C, compared to 15^{o}C in titanium. Microscopic examination of polished and quenched samples showed a rumpled surface (Fig. 25) but the rumpling was not so pronounced as in titanium. The critical cooling rate for zirconium(300^{o}C/sec.) is found to be higher than for titanium, and the Ms measured was 860^{o}C. Duwez[3] reported a value of 850^{o} C which is again low in comparison

to the result of this investigation. However, these results and those of Duwez agree that the depression of the transformation temperature is much less in zirconium than in titanium. Kaufmann[67] in his thermodynamic calculations on the titanium-zirconium system showed the driving force for martensite in dilute zirconium base alloys and zirconium ($\sim$ 60 cal/mol) to be higher than in titanium ($\sim$ 40 cal/mol). On this basis, and if a 20 cal/mol difference is significant, one would except the difference in equilibrium temperature and Ms temperature in zirconium to be more than in titanium, which is contrary to the results obtained. However, measurement of electrochemical potential difference between equiaxed zirconium and martensitic zirconium implied a free energy difference of 29 $\pm$ 5 cal/mol which is less than in titanium (48 $\pm$ 10 cal/mol). Considering the free energy difference between equiaxed and martensitic structures in iron[68], titanium and zirconium and the corresponding depression in their transformation temperature the present result on zirconium could be justified to be correct.

Studies on iron show transformation temperatures of 912^{0}C and 517^{0}C on slow cooling and on quenching, respectively, with a total depression of 395^{o}C at quenching rates above 5500^{o}C/sec. This confirms the results reported by Esser et al.[18] of 905^{o}C and about 500^{o}C respectively, for the two transformation temperatures. As indicated earlier in this thesis, these values agree with the transformation temperature of 910^{o}C, and with the Ms value for pure iron of 520^{o}C (extrapolated to zero carbon from steel data[19].

The critical cooling rate required to suppress the diffusion type of transformation appears to be of the order of 5500°C/sec. Duwez[3] in his work on pure iron observed the transformation temperature to be depressed to only 750°C at a cooling rate of 10,000°C/sec.

A similar behaviour was noticed by the author of this thesis with iron containing impurities of C, Mn, P, S, Si, Ni , Cr, V, Mo, Cu, Al, N, O, H, Pb (adding up to a total of 0.1% approximately) with cooling rates up to 10,000°C/sec. Two transformation temperatures in the range of 750-700°C and 530-515°C were recorded. In view of the above observation it appears that the disagreement lies in the difference in the purity of the iron used by the investigators.

The work of Owen[69] implies a transformation at a temperature between Ms and To in iron, which is suggested to be a massive transformation[70] occuring at rates of cooling sufficient to inhibit the diffusion transformation and at the same time inadequate to drive the martensitic reaction. The massive transformation is considered to be a diffusionless transformation in the sense that it proceeds by a very rapid movement of high energy incoherent grain boundaries, but no bulk diffusion takes place. However, it also implies that the lattice transformation takes place by movement of an array of dislocations (grain boundaries). This rules out the diffusionless process . Further it is said that the product of massive transformation does not bear any definite crystallographic relation to the parent phase, which again suggests a different mechanism to a diffusionless reaction.

Since the concept of the massive transformation is very recent, no further comments can be made at this time.

A preliminary experiment on the measurement of the free energy difference between ferrite and martensite in pure iron was recently conducted by Singh and Parr[68]. The electrochemical potential difference measured at room temperature between equiaxed ferrite and martensite (both in pure iron) implied a free energy difference of 300± 70 cal/mol. This is much the same as the calculated value[50] for the driving force of the martensite reaction in iron carbon alloys- although it is appreciated that this value is at room temperature while the other is at Ms.

It appears that the driving force of the martensite reaction in iron and possibly in iron carbon alloys is simply the amount of free energy representing the difference between equiaxed ferrite and martensite in pure iron. In other words, considering iron martensite a phase that is amenable[68] to thermodynamic treatment, it is in " equilibrium" with iron ferrite at the Ms temperature where $F_{\alpha} = F_{M}$.

This is a different concept to that generally held about martensite transformations, and it would be premature to appraise its validity.

Similar measurement of electrochemical potential difference between martensite and equiaxed structure in titanium im-

plied a value of 48 $\pm^{10}$ cal/mol*, which again equals the calculated value[67] of the driving force of martensite in titanium base alloys.

From the above observations on titanium, zirconium and iron, it is very evident that the driving force of the martensite reaction in titanium and titanium base alloys is much less than in iron binary alloys. The possible explanation could be given in terms of strain and surface energies only, if other factors are negligible. The strain and surface energies associated with the transformation are dependent on the following factors[28].

(a) The shear modulus of the metal.

(b) The homogeneous shear strain associated with the transformation.

(c) The heterogeneous strain or dislocation spacing in the high temperature phase and martensite interface.

The transformation strain energy depends upon (a) and (b) while the surface energy depends upon (a) and (c). Both the surface and strain energies tend to oppose the transformation and the driving force must be greater than or equal to the sum of the surface and strain energies in order that the reaction proceed.

The shear modulus of iron base alloys is about four times that of titanium. The homogeneous strain is shown to be almost the same in both the cases[67]. Frank's[71] analysis indicates that heterogeneous strain in steels can be described by having the aus-

---

* See Appendix IV.

tenite- martensite interface composed of screw dislocations: this gives a large interfacial energy. MacKenzie & Bowles[72] have analysed the crystallography of the martensite transformation in titanium and suggested that the transformation can be accomplished by almost total homogeneous strain, involving very small heterogeneous strain. Thus the interfacial energy of $\beta \rightarrow \alpha'$ transformation will be small. The combination of these factors indicates that the " backing stress " (i.e. the sum of the surface and strain energies[28]) will be much smaller in titanium than in iron-base alloys. Further, a large number of parallel striations are observed in α' plates of martensite in titanium and titanium-copper alloys (Figs. 35 and 36). It implies that the martensite transformation in titanium grows by twinning of the α' plate (c.p.h.) itself. Cahn[73] has already shown similar α' plates in uranium twin readily, and suggests that the transformation stresses are relieved by twinning of the α' plate: the plate grows with ease, requiring a small driving force. In iron the martensite (b.c.c.) plate forms in a ductile matrix of austenite (f.c.c.) and the transformation stresses are relieved by simultaneous deformation of the matrix. The twinning stress of a c.p.h. lattice of titanium would be much less than the deformation stress of austenite (f.c.c.) . This appears to take into account the large difference in the driving force of martensite in iron and titanium.

In view of the deformation associated with martensite transformation, Bilby and Christian[26] gave a proposal that martensite in steel probably forms also by twinning. They described a model

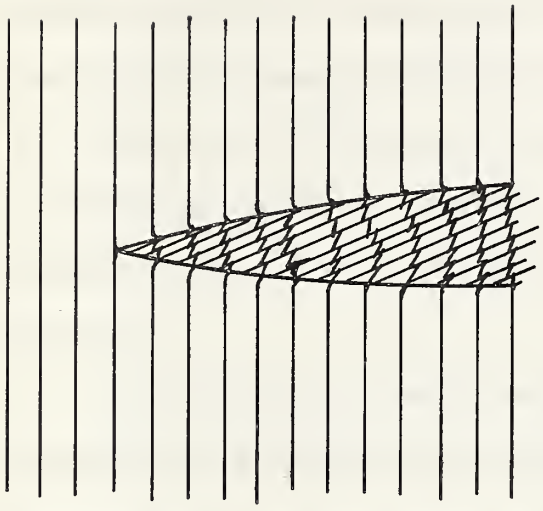

Titanium Martensite growth without slip in β matrix but with twinning in α' plate permitting shear adjustment.

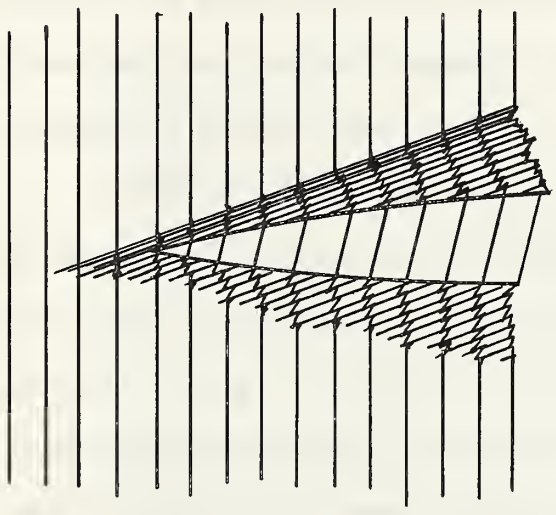

Steel Martensite growth with slip in matrix; permitting shear adjustment.

Fig. 37

MORPHOLOGY OF MARTENSITE TRANSFORMATION

by which the deformation occuring in steel martensite could be met by twinning only. However, such twins as they describe, of equal size and opposite orientation will result in zero total shape deformation in steel. They further suggested that the observed shape deformation in steel would be a result of the ratio of the two twin thicknesses. From the geometry of the martensite needle in steels, the two halves of the martensite needle appear to be equal and opposite in character, and the model seems to be inadequate to account for shape deformation observed in steel martensites.

Recent analysis of the crystallography of the martensitic transformation follows the Greninger and Troiano[74] concept of deformation. The total shape deformation is suggested to be a result of a two-stage process involving a hypothetical intermediate lattice. The two stages are the homogeneous and the inhomogeneous deformation.

Frank[71] visualized a screw dislocation to be operative at the transformation front and suggested that the deformation occuring simultaneously with the transformation could easily give the homogeneous shear. He also showed that a similar screw dislocation operating at the surface of the γ and primary martensite lattices could transform γ completely into martensite.

Electron microscopic studies on martensite in plain carbon steels by Kelly and Nutting[75] have shown two different morphologies for high and low carbon steels. The high carbon ($>$ 0.34 C)

MICROSTRUCTURES

Fig. 38 Mechanical twinning in α titanium x 300, etchant HF + HNO_3 + glycerine

Fig. 39 Twin free α titanium x 300, etchant HF + HNO_3 + glycerine

MICROSTRUCTURE

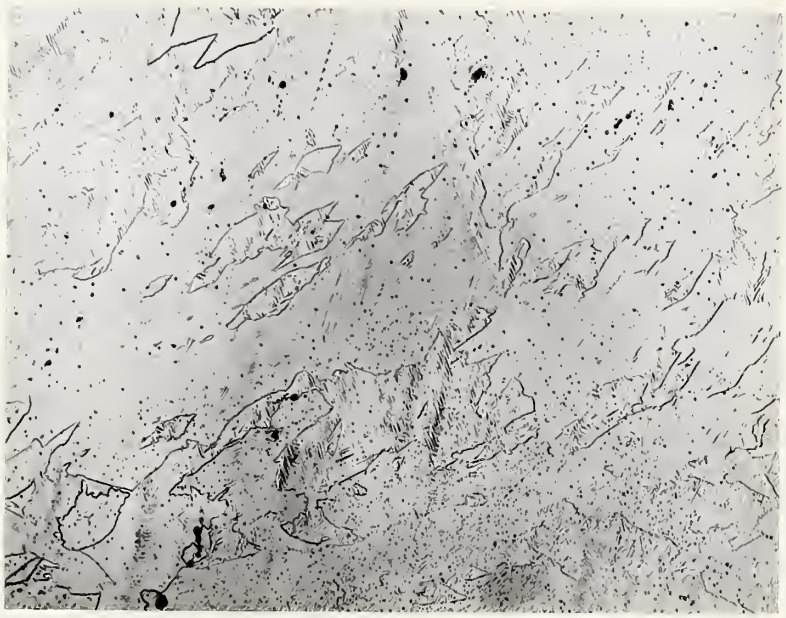

Fig. 40 Quenched, polished and etched titanium x 150, etchant HF + HNO_3 + glycerine

steel martensites have shown fine twinning in the martensite plates, while this twinning was not observed in low carbon steels. Kelly and Nutting suggested that the possible difference is due, first, to the increased stacking fault energy with increased carbon content and second to the temperature dependence of the crystal morphology. It appears that in the iron-carbon system there is a temperature above which twinning cannot occur. Thus the high carbon steels having Ms below this temperature may transform by twinning. However, no quantitative determinations of maximum twinning temperatures have been made.

A slowly cooled titanium sample is very sensitive to mechanical twinning. Fig. 38 shows a titanium sample in the polished and etched condition. A large amount of twinning is present throughout the sample, but the same sample carefully polished under light pressure showed an almost twin free structure (Fig. 39). This implies that the α phase in titanium is very easily deformed by twinning—a common feature of close packed hexagonal metals.

A quenched, polished and etched sample of titanium under the microscope does not appear to be very much different to a slowly cooled sample. However, it is not so very sensitive to mechanical twinning. Neverthless, all the pure titanium martensite samples examined showed permanent, fine striations at certain confined regions (Fig. 40) which presumably arise from twinning during the martensite transformation.

Summary and Conclusions

1. There are two different mechanisms operative with phase transformation in titanium, zirconium, titanium-zirconium alloy and titanium-copper alloys. The one operative at lower rates of cooling is a process of nucleation and growth by diffusion and the other operative at higher rates of cooling is a shear type process called " Martensitic "

2. Iron also transforms martensitically at cooling rates above 5500°C/sec, at a temperature of 517 ± 4°C.

3. The $\gamma \rightarrow \alpha$ transformation in iron on slow cooling rates is a diffusion process.

4. The Ms temperatures of titanium, zirconium, titanium-43 pct. zirconium alloy are determined to be 868, 860 and 497 ± 4°C respectively. The corresponding critical cooling rates are 200, 300 and 60°C/sec.

5. The Ms temperatures of titanium-copper alloys progressively decrease with increasing copper content. The Ms temperatures of 0.5, 1.0, 1.5, 3.0 and 5.2 pct. copper alloys are 857, 842, 827, 745 and 625 ± 4°C respectively and the corresponding critical cooling rates are 200, 150, 120, 120 and 900°C/sec.

6. The transformation in 8 pct. copper alloy at quenching rates is possibly martensitic at a temperature of approximate-

ly 460°C. No retained β has been detected at cooling rates of up to 3000°C/sec.

7. The martensite reaction in titanium, zirconium, titanium-zirconium alloy and titanium copper alloys occurs at a much smaller depression below the equilibrium temperature than the martensite transformation in iron. This implies a lower driving force in titanium, zirconium and their alloys compared to iron— assuming the general concept of " driving force " to be applicable.

8. A possible difference in the morphology of the martensite transformation in titanium, zirconium and titanium alloys on one hand and in iron on the other hand, is suggested to account for the large difference in the two driving forces. The martensite transformation in titanium, zirconium and titanium alloys proceeds by twinning of the martensite plate itself, while in iron the martensite transformation proceeds by simultaneous deformation of the ductile austenite matrix.

9. In titanium-copper alloys, the hardness of the nucleation and growth product (diffusion) increases with increasing copper content. The rate of increase of hardness declines with increasing copper content; beyond 5.2 pct. copper (eutectoid composition) the increase is small.

10. The martensite structure of titanium-copper alloys is

harder than the corresponding diffusion product. The martensitic hardnesses rise sharply with initial addition of copper and the rate declines with increasing copper content. The increase in hardness is probably due to the strains associated with the martensite transformation.

11. α titanium is very sensitive to mechanical twinning.

12. The free energy differences between the α structures and the martensitic structures of titanium and of zirconium have been measured to be 48 $\pm$ 10 and 29 $\pm$ 5 cal/mol. respectively at room temperature. A comparison of these values with the corresponding value for iron (300 cal/mol.) permits a tentative thought to be proposed in which " driving force " as the excess free energy required by martensite over ferrite loses significance. A suggestion is made, instead, that martensite be considered a phase in its own right and that the $A \longrightarrow M$ transformation occurs when the free energies of austenite and martensite are equal.

BIBLIOGRAPHY

1. Lamborn, I.R; J. Austrialian Institute of Metal, Aug. 1960, Vol.5., No.2, P. 140.

2. Troiano, A.R. and Greninger, A.B.; Metal Progress. Aug. 1946, Vol.50, P.303.

3. Duwez, P.; Trans. A.I.M.M.E., 1951, Vol. 191, P.765.

4. Pietrokowsky, P. and Duwez, P.; Trans. A.I.M.M.E. 1952 Vol. 194, P.627.

5. Duwez, P.; Trans. A.S.M., 1953, Vol.45, P. 934.

6. Holden, F.C., Watts, A.A., Ogden, H.R. and Jaffee.R.I.; Trans. A.I.M.M.E., 1955, Vol.203, P. 117.

7. Joukainen, A., Grant, N.J. and Floe, C.F.; Trans. A.I.M.M.E. 1952, Vol. 194, P. 766.

8. Mc Quillan, A.D.; Journal Inst. Met. 1950-51, Vol. 78, P.249.

9. Mc Quillan, A.D.; Nature, 1949, Vol.164, P.24.

10. Mc Quillan, A.D.; Proc. Roy. Soc., 1950, Vol.A 204, P.309.

11. Williams, A.J., Cahn, R.W. and Barrett, C.S.; Acta Met. 1954, Vol. 2, P. 117.

12. Wiskel, S.J., Youdelis, W.V. and Parr, J.G. Trans. A.I.M.E., 1959, Vol. 215, P. 875.

13. Burgers, W.G.; Physica. 1934, Vol. 1, P. 561.

14. Newkirk, J.B. and Geisler, A.H.; Acta Met. 1953, Vol. 1, P. 370.

15. Mc Hargue, C.J.; Acta Cryst., Camb. 1953, Vol. 6. P. 529.

16. Hayes, E.T. and Kaufmann, A.R.; Symposium A.S.M., Zirconium alloys. Cleveland, 1953, 161.

17. Gaunt, P. and Christian J.W.; Acta Met. Aug. 1959, Vol. 7. P. 534.

18. Esser, H. Elender, W. and Spenel, E.; Archiv für der Eisenhütten wesen, 1933, Vol. 6, P. 389.

19. Greninger, A.B.; Trans. A.S.M. 1942, Vol. 30, P. 1.

20. Duwez, P.; Journal Institute of Metals, 1951-52, Vol. 80, P. 525.

21. Fogel, A.A.; IZV, Akad Nauk SSSR, OTN. Metall. 1 Topl., 1959, No. 2, P. 24-34.

22. Polonis, D.H. and Parr, J.G.; Trans. A.I.M.M.E. May 1956, P. 514.

23. Guinier, A.; Substructures in crystals, " Imperfection in nearly perfect crystals " , 1952, New York, John Willy & Sons Inc., P. 402.

24. Mott, N.F.; Proceedings Physical Soc., London (1951), B 64, P. 729.

25. Gomez, M.P and Polonis, D.H.; Trans. A.S.M. 1960, Vol.52, P. 201.

26. Bilby, B.A. and Christian, J.W.; "The Mechanism of Phase Transformation in Metals," Institute of Metals Monograph and Report Series, 1955, No. 18, P. 121.

27. Cohen, M.; "Phase transformations in solids," John Wiley & Sons, New York; Chapman and Hall; London 1951, P. 588.

28. Kaufmann, L. and Cohen, M.; Progress in Metal Physics, Pergamon Press, London 1958, Vol. 7, P. 165.

29. Averbach, B.L. and Cohen, M; Trans. A.S.M. 1949, Vol. 41, P 1024.

30. Das Gupta, S.C. and Lement, B.S.; Trans. A.I.M.M.E, 1951, Vol. 191, P. 727.

31. Machlin, E.S. and Cohen, M., Trans. A.I.M.M.E. 1952, Vol. 194, P. 489.

32. Kulin, S.A. and Speich G.R.; Trans. A.I.M.M.E. 1952, Vol. 194, P. 258.

33. Holden, A. N. ; Acta Met. 1953, Vol. 1; P. 617.

34. Shih, C.H., Averbach, B.L. and Cohen, M; Trans. A.I.M.M.E. 1955, Vol. 203, P. 183.

35. Kurdjumov, G.V. and Maksimova, O.P.; Dokl. Akad. Nauk SSSR 1948, Vol. 61, P. 83.

36. Kurdjumov, G.V. and Maksimova, O.P. ; Dokl. Akad. Nauk SSSR 1950, Vol.73, P. 95.

37. Kurdjumov, G.V. and Maksimova, O.P.; Dokl. Akad. Nauk SSSR 1951, Vol. 81, P. 565.

38. Machlin, E.S. and Cohen, M.; Trans. A.I.M.M.E. Sept. 1951, Vol. 191, P. 746.

39. Chang, L.C. and Read, T.A.; Trans. A.I.M.M.E. 1951, Vol. 191, P.47.

40. Bukart, M.W. and Read, T.A.; Trans. A.I.M.M.E., 1953, Vol. 197, P. 1516.

41. Basinski Z.S. and Christian, J.W.; Acta Met. 1954, Vol. 2, P. 148.

42. Bowles, J.S.; Barrett, C.S., and Guttmann, L.; Trans. A.I.M.M.E., 1950, Vol. 188, P. 1478.

43. Basinski, Z.S. and Christian, J.W.; J. Inst.Metals, 1951-52, Vol. 80, P. 659.

44. Kurdjumov, G.V. and Khandros, L.G.; Doklady Akad. Nauk SSSR, 1949, Vol. 66, P. 211.

45. Bowles, J.S. and Barrett, C.S.; Progress in Metal Physics, Pergamon Press Ltd., London, 1952, Vol. 3, P.1.

46. Fisher J.C., Hollomon, J.H and Turnbull, D.; J. App. Phy. 1948, Vol. 19, P. 775.

47. Fisher J.C., Hollomon, J.H. and Turnbull, Trans, A.I.M.M.E. 1949, Vol. 185, P. 691.

48. Fisher, J.C.; Acta Met. 1953, Vol. 1, P. 32

49. Machlin, E.S. and Cohen, M.; Trans. A.I.M.M.E. 1951, Vol. 191, P. 1019.

50. Cohen, M., Machlin, E.S. and Paranjpe, V.G.; " Thermodynamics in Physical Metallurgy " A.S.M. 1952, P. 242.

51. Machlin E.S. and Cohen, M.; Trans. A.I.M.M.E. 1952, Vol. 194, P. 519.

52. Averbach, B.L., Cohen, M. and Fletcher, S.G. Trans A.S.M.(1948), Vol. 40, P. 728.

53. Kurdjumov, G.V.; Zhur. Tekhn. Fiz. 1948, Vol. 18, P. 999. Problemy Mettalovedeniya if fiziki metallov 1949, Vol. 1, P. 132.

54. Philibert, J. and Crussard, c, J. Ironand steel Inst. London, May 1955.

55. Kaufmann, L. and Cohen, M., Trans. A.I.M.M.E. 1956, Vol. 206, P. 1393.

56. Kulin, A., Cohen, M. and Averbach, B.L.; Trans. A.I.M.M.E. 1952, Vol. 4, P. 661.

57. Troiano, A.R. and Mc Guire, F.T.; Trans. A.S.M., 1943, Vol. 31, P. 340.

58. Greninger, A.B.; Trans. A.I.M.M.E. 1939, Vol. 133, P. 204.

59. Greninger, A.B. and Mooradian, V.G.; Trans, A.I.M.M.E. 1938, Vol. 128, P. 337.

60. Reynolds, J.E. and Bever, M.B.; Trans. A.I.M.M.E. 1952, Vol. 194, 1065.

61. Hiltz, R.H.; Trans. A.I.M.E., Feb. 1959, Vol. 215, P. 138.

62. Bumm, H. and Dehlinger, U.; Metalkunde 1937, Volume 29, P. 29.

63. Wassermann, G.; Metallwirtschaft, 1934, Vol. 8, P. 133.

64. Obinate, I. and Hayashi, M; J. Iron Steel Inst. Japan, 1937, Vol. 23, P. 1092.

65. Barrett, C.S. and Trautz, O.R.; Trans. A.I.M.M.E. 1948, Vol. 175, P. 579.

66. Troiano, A.R. and Tokich, J.L.; Trans. A.I.M.M.E. 1948, Vol. 175, P. 728.

67. Kaufmann, L.; Acta Met. Aug. 1959, Vol. 7, P. 575.

68. Singh, K.P. and Parr, J.G.: Acta Met. (in Publication)

69. Owen, W.S.; (Dept. Metallurgy, University of Liverpool, England); private communications.

70. Massalski, T.B.; Acta Met., April 1958, Vol. 6. P. 243.

71. Frank, F.C.; Acta Met. 1953, Vol. 1, P. 15.

72. MacKenzie, J.K. and Bowles, J.S.; Acta Met., 1957, Vol.5, P. 137.

73. Cahn, R.W., Acta Met. 1953, Vol. 1, P. 49.

74. Greninger, A.B. and Troiano, A.R.; Trans. A.I.M.M.E., 1949, Vol. 185, P. 590.

75. Kelly, P.M. and Nutting, J.; J. Iron and Steel Inst. 1961, Vol. 197, Part 3, P. 199.

TABULATIONS OF TRANSFORMATION TEMPERATURES ON COOLING

APPENDIX I

TABLE 2

Transformation temperatures of as received pure titanium*

Cube sample — Soaking temperature 995 ± 5°C

Cooling rate °C/sec (Measured at 900°C)	Transformation temp. oC.	Cooling rate °C/sec (Measured at 900°C)	Transformation temp. °C
10	887	1.5	886
15	869	1.8	887
30	867	20	887
35	866	49	875
40	867	96	880
75	866	104	884
90	868	116	883
93	868	120	884
4000	867	138	876
4100	867	144	883
		430	869
4100	867	460	867
		4800	868
		5700	868
		5900	868
		6600	868

* See Appendix V for composition of the materials.

TABLE 3

Transformation temperatures of remelted* pure titanium

Cube sample — Soaking temperature 995 ± 5°C

Cooling rate °C/sec (Measured at 900°C)	Transformation temp. °C	Cooling rate °C/sec (Measured at 900°C)	Transformation temp. °C
1.5	890	1.5	886
4.5	890	1.5	887
10	887	5	887
20	888	20	875
40	887	50	875
50	888	96	880
90	868	104	884
93	868	116	883
112	887	120	884
4000	868	138	876
4100	867	144	883
4100	867	434	869
		460	867
		4800	868
		5700	868
		5900	868
		6600	868

* by levitation melting[21] in argon

TABLE 4

Transformation temperatures of remelted pure titanium

Ring sample — Soaking temperature 995 ±5°C

Cooling rate °C/sec (Measured at 900°C)	Transformation temp. °C	Cooling rate °C/sec (Measured at 900°C)	Transformation temp. °C
2	890	1	887
18	883	3	887
44	885	40	888
76	883	70	887
150	874	80	887
350	868	118	888
940	863	594	863
1460	864	800	862
1470	865	950	866
		1050	863
		1500	862
		1560	862

TABLE 5

Transformation temperatures of titanium-copper alloys

0.5 pct. Copper		1.0 pct. Copper	
Soaking temperature 990 ± 5°C		Soaking temperature 995 ± 5°C	
Cooling rate °C/sec (Measured at 900°C)	Transformation temp. °C	Cooling rate °C/sec (Measured at 900°C)	Transformation temp. °C
4	885	2	875
20	872	6	860
60	868	25	866
135	870	65	858
150	867	120	846
210	858	140	846
840	858	160	849
920	856	220	841
5190	857	850	842
6110	857	1450	843
6110	856	1650	843
		2190	838
		2220	839
		2900	843
		4060	838
		5600	843

TABLE 6

Transformation temperatures of titanium-copper alloys

1.5 pct Copper		3 pct. Copper	
Soaking temperature 990 ±5°C		Soaking temperature 990 ± 5°C	
Cooling rate °C/sec (Measured at 900°C)	Transformation temp. °C	Cooling rate °C/sec (Measured at 900°C)	Transformation temp. °C
5	868	4	818
18	857	20	818
60	842	38	785
105	838	78	768
126	830	103	744
126	827	130	748
170	829	220	752
210	829	890	743
410	825	915	752
720	821	1200	745
1100	830	1370	753
1130	839	2100	742
2800	826	4400	742
2800	825	6700	742
7200	825	8800	743

TABLE 7

Transformation temperatures of titanium-copper alloys

5.2 pct. Copper		8.0 pct. Copper
Soaking temperature 990 ±5°C		Soaking temperature 990 ±5°C
Cooling rate °C/sec (Measured at 800°C)	Transformation temp. °C	
2.6	805	
5	795	
21	759	
27	764	No Martensite transformation
60	742	temperature observed.
72	750	
103	728	
110	729	
129	741	
360	670	
430	662	
1400	622	
2500	630	
3600	628	
3900	624	

TABLE 8

Transformation temperatures of zirconium and titanium- 43 pct. zirconium alloy

Zirconium		Ti- 43pct Zr alloy	
Soaking temperature 990±5°C		Soaking temperature 690±5°C	
Cooling rate °C/sec (Measured at 900°C)	Transformation temp. °C	Cooling rate °C/sec (Measured at 550°C)	Transformation temp. °C
3	867	1.8	540
5	867	2	542
18	867	3	543
48	863	8.8	530
78	863	24	518
100	863	31	507
110	863	35	501
200	861	37	505
500	860	41	502
1600	860	49	498
1700	860	177	497
4300	860	247	521
4600	860	750	500
6300	860	810	500
		1480	486
		2900	492
		4300	493
		7900	492

TABLE 9

Transformation temperatures of Iron

Cube sample — Soaking temperature 980 ± 5°C

Cooling rate °C/sec (Measured at 950°C	Transformation temp. °C
1.5	910
3	912
2	912
2250	547
4600	531
5300	517
6500	518
6900	517
10000	517

TABLE 10

Depression of Martensite Temperatures
Below Equilibrium Temperatures

Metal	(To - Ms) in °C	Alloy	(To - Ms) in °C
Titanium* (Cube sample)	15	Ti- 0.5 pct. Cu	17
Titanium (Ring sample)	20	Ti- 1.0 pct. Cu	24
Zirconium*	7	Ti- 1.5 pct. Cu	31
Iron*	395	Ti- 3.0 pct. Cu	88
		Ti- 5.2 pct. Cu	173
		Ti- 43 pct. Zr	53

* See Appendix V for composition of the material

SUMMARY OF THE TRANSFORMATION TEMPERATURES ON REHEATING QUENCHED SPECIMENS

APPENDIX II

TABLE 11

Transformation temperatures on reheating quenched titanium, zirconium, and Ti-Zr alloy

Titanium		Zirconium	
Heating rate °C/sec (Measured at 800°C)	Transformation temp. °C	Heating rate °C/sec (Measured at 800°C)	Transformation temp. °C
15	892	7	886
20	896	31	868
25	890	35	867
26	896	40	868
28	890		
33	895		
45	892		
55	895		

Ti- 43 pct. Zr Alloy

Heating rate °C/sec (Measured at 450°C)	Transformation temp. °C
18	507
31	498
32	505
35	506
90	497

TABLE 12

Transformation temperatureson reheating quenched titanium-copper alloys

0.5 pct Copper		1.0 pct. Copper	
Heating rate °C/sec (Measured at 800°C)	Transformation temp. °C	Heating rate °C/sec (Measured at 800°C)	Transformation temp. °C
19	878	16	875
32	872	19	877
33	873	22	873
35	869	41	875
42	872	48	879
		50	873

TABLE 13

Transformation temperatures on reheating quenched titanium-copper alloys

1.5 pct. Copper		3.0 pct. Copper	
Heating rate °C/sec (Measured at 800°C)	Transformation temp. °C	Heating rate °C/sec (Measured at 750°C)	Transformation temp. °C
72	839	35	800
78	834	55	797
80	834	58	790
		62	793
		62	793
		62	790
		98	804

TABLE 14

Transformation temperatures on reheating quenched titanium-copper alloys

5.2 pct. Copper

Heating rate °C/sec (Measured at 750°C	Transformation temp. °C
10	775
17	775
31	802
38	800
43	799
65	798
100	797

SUMMARY OF THE HARDNESS RESULTS

ON TITANIUM AND Ti-COPPER ALLOYS

APPENDIX III

TABLE 15

Alloy	Slow cooling 1.5-3°C/sec Hardness in VPN	Quenched 2000-4000°C/sec Martensite Hardness in VPN
Ti - pure	77 (as received) 78 (remelted)	94
Ti - 0.5 pct. Copper	132	163
Ti - 1.0 pct. Copper	154	206
Ti - 1.5 pct. Copper	172	250
Ti - 3.0 pct. Copper	232	278
Ti - 5.2 pct. Copper	263	348
Ti - 8.0 pct. Copper	289	x

ELECTROCHEMICAL MEASUREMENTS ON TITANIUM AND ZIRCONIUM

APPENDIX IV

TABLE 16

Measurement on E. M. F. Difference in α Titanium and α' (Martensitic) Titanium Electrodes in Titanous Chloride Solution*

Temp. °C Sample I		Diff. in E. M. F. in millivolt	Temp. °C Sample II		Diff. in E. M. F. in millivolt
28	0 hr.	2.1	Solution I		
28	10 min.	0.7	26	0 hr.	0.5
28		0.8	26		0.45
28		0.7	26		0.65
28	3 hrs.	0.5	26		0.65
28		0.7	26	1 hr.	0.6
28		0.7	26	13 hrs.	0.7
28		0.7	26		0.7
28		0.7	26		0.7
28		0.8	26		0.7
26	26 hrs.	0.8	25		0.8
26		0.8	26		0.7
26		0.7	26		0.7
27		0.7	26	27 hrs.	0.7
28		0.7			
28		0.7	Solution II		
28		0.7	26	0 hr.	0.5
28		0.7	26		0.45
28		0.7	26		0.6
28		0.7	26		0.8
28		0.65	26		0.8
28	30 hrs.	0.7	23		0.85
			23		0.8
			25	4 hrs	0.7
			25	20 hrs	0.7

* The solution contained 0.05 M (approx.) each of $TiCl_3$, HCl and EDTA compound in doubly distilled and degassed water (degassed by bubbling helium).

TABLE 17

Measurement on E.M.F. difference in α zirconium and α' (Martensitic) zirconium electrodes in dilute $Zr_2(SO_4)_3$*

Temp. °C		Diff. in E.M.F. in millivolt	Temp. °C		Diff. in E.M.F. in millivolt
Solution I			23		0.45
21	0 hr.	3·1			
21	7 hrs.	0.45	23		0.45
21	19 hrs.	0.35	23	2 hrs.	0.4
21		0.45	24		0.1
21		0.4	23		0.35
21		0.35	24.5	6 hrs.	0
22		0.4	24	6 hrs.10 min.	0.15
22		0.45	24	7 hrs.	0.4
22		0.45	24		0.4
22		0.35	24	20 hrs.	0.4
22		0.4	Solution III		
22		0.45	22	0 hr.	0.6
22		0.5	23		0.3
23	24 hrs.	0.45	23	2 hrs.	0.4
Solution II			23		0.4
23	0 hr.	3·0			
23	30 min.	0.4	23		0.45
23		0.45	23		0.45
			23		0.4
			23	19 hrs.	0.45

* 0.05M solution (approx) prepared in doubly distilled, degassed water with few drops of concentrated H_2SO_4.

Calculations:

The electrode reactions are

$$Ti \rightleftharpoons Ti^{+++} + 3e, \text{in titanium}$$

and

$$Zr \rightleftharpoons Zn^{+++} + 3e, \text{in zirconium}$$

at both the electrodes of martensitic and equiaxed structure in titanium and in zirconium.

Then, the free energy difference (in joules) between the electrodes wil = nEF, where

n = number of electrons taking part in the reaction

E = measured E. M. F

F = (96,500), the Faraday's number in coulumbs.

(1) Titanium $E = 0.7 \pm 0.15$ mv

$$\triangle F = 3 \times E \times 22980$$

$$= \frac{3 \times 0.7 \times 22980}{1000}$$

$$= 48 \pm 10 \text{ cal/mol}$$

(2) Zirconium $E = 0.42 \pm 0.05$

$$\triangle F = \frac{3 \times 0.42 \times 22980}{1000}$$

$$= 29 \pm 5 \text{ cal/mol}$$

MATERIALS USED IN THE PROJECT

APPENDIX V

Titanium

From - Foote Mineral Company, Pennsylvania

Analysis - Si - .004 pct (by wt.)

Al - .003

Mg - .005

Mn - .008

Fe - .002

Cr - Traces

Ni - Traces

Sn - .006

Cu - .002

Ca - .008

Mo - N. D.

Zr - $<$ .05

Balance - Titanium

Copper

From - Johnson Matthey & Co. Ltd., London

Analysis - Si - 3 parts/million

(Fe, Pb, Ni) - 2 parts/million

Ca, Mg, Mn, Ag - 1 part/million each

Oxygen - $<$ .01 pct

Zirconium

From - Foote Mineral Company, Pennsylvania

Analysis - Zr + Hf - 99.83 pct (by wt.)

Hf/Zr x 100	- 2.03
Al	- .005
Cr	- .002
Ca	- .05
Cu	- .0003
Fe	- .003
Mn	- .001
Mg	- .01
Mo	- Traces
Ti	- .008
Sn	- .035
Si	- .05

Iron

From - Department of Mining and Metallurgy
University of British Columbia, Vancouver, B.C.

Analysis* -

C	-	.005 pct (by wt.)
Mn	-	Traces
S	-	Nil
Si	-	.02
Ni	-	.06
Cr	-	Nil
Cu	-	Nil

* Analysis done by Coast Testing Laboratory Ltd., Vancouver, B.C.

B29795